Kirk-Othmer Encyclopedia of Chemical Technology.

XYLYLENE POLYMERS

In a process capable of producing pinhole-free coatings of outstanding conformality and thickness uniformity through the unique chemistry of *p*-xylylene (PX) [502-86-3] (**1**), a substrate is simply exposed to a controlled atmosphere of pure gaseous monomer. The coating process is best described as a vapor deposition polymerization (VDP). The monomer molecule is thermally stable, but kinetically very reactive toward polymerization with other molecules of its kind. Although it is stable as a rarified gas, upon condensation it polymerizes spontaneously to produce a coating of high molecular weight, linear poly(*p*-xylylene) (PPX)[25722-33-2] (**2**). This article emphasizes recent VDP developments. There have been several reviews of the subject (1), which offer a more thorough treatment of early developments in the field.

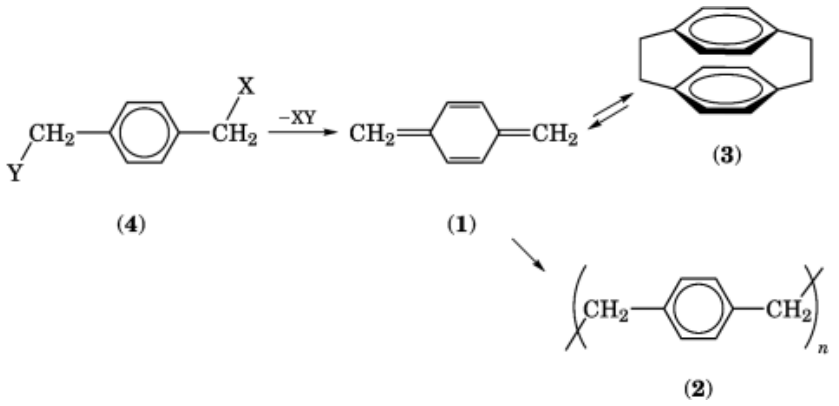

In the commercial Gorham process (2), the extremely reactive PX is conveniently generated by the thermal cleavage of its stable dimer, *cyclo*-di-*p*-xylylene (DPX), a [2.2]paracyclophane [1633-22-3] (**3**). In many instances, substituents attached to the paracyclophane framework are carried through the process unchanged, ultimately becoming substituents of the polymer in the coating.

The process takes place in two stages that must be physically separate but temporally adjacent. Figure 1 presents a schematic of a typical parylene deposition process, also indicating the approximate operating conditions.

The PPXs formed as coatings in the Gorham process are referred to generically as the parylenes. The terms Parylene N [25722-33-2], Parylene C [9052-19-1], and Parylene D [52261-45-7] refer specifically to polymers produced as coatings by the Gorham process using the dimers DPXN, DPXC [28804-46-8], and DPXD [30501-29-2], respectively, originally marketed by Union Carbide Corporation.

The parylene process has certain similarities with vacuum metallizing. The principal distinction is that truly conformal parylene coatings are deposited even on complex, three-dimensional substrates, including on sharp points and in hidden or recessed areas. Vacuum metallizing, on the other hand, is a line-of-sight coating

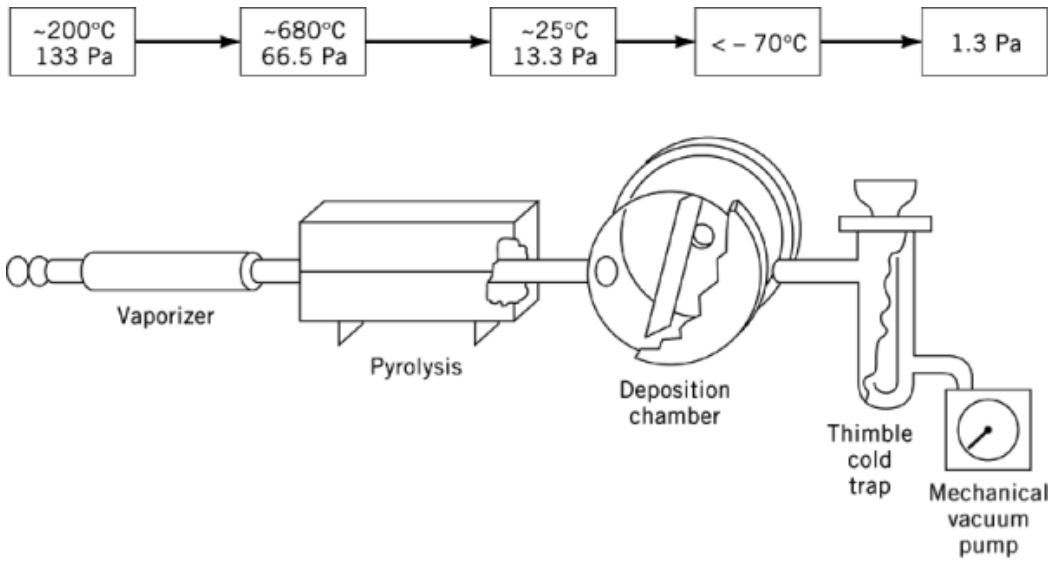

Fig. 1. Parylene deposition apparatus. To convert Pa to torr, multiply by 0.0075.

technology. Whatever areas of the substrate cannot be "seen" by the evaporation source are "shadowed" and remain uncoated (see Vacuum technology).

The *p*-xylylene species plays a central role in the coating process itself as well as in the making of the dimers which are used as feedstocks for the coating process. Polymers and dimers have both been made from precursor *p*-xylene compounds (**4**) featuring a variety of X and Y leaving groups. The conditions of the reaction determine the relative amounts of the resulting dimeric or polymeric products. Dilution is of course the key element in any procedure which offers a high yield of dimer.

The modest commercial success the *p*-xylylene dimer-based Gorham process has achieved to date is readily attributed to the fact that thermal cleavage of cyclic dimer produces the *p*-xylylene monomer in essentially quantitative yield, while at the same time producing no gaseous by-products. In a gas-to-solid coating process, any gaseous entities generated from the leaving groups X and Y, necessarily formed in volumes comparable to the volume of the monomeric *p*-xylylene generated, would at the very least need to be exhausted through the pumping system, thereby slowing the process down. Moreover, certain of the most effective leaving groups XY, such as halogens or halogenide acids, would create a corrosion hazard both for any sensitive substrates to be coated and for the deposition equipment itself.

1. Gorham Process Monomers

The eight-carbon monomer PX is generated in the first stage of the parylene process by heating gaseous dimer as it passes through a high temperature zone. Its intermediacy in the process was deduced by the earliest investigators. Apprehending the unusual properties of PX is an important aid to understanding the unique features of the coating process.

1.1. Chemical Evidence for PX Monomer

Establishing early on that PX is indeed the pyrolysis product, rather than the molecule formed by breaking only one of the original dibenzyl bonds, the dimer diradical (**5**), would prove to be an important development.

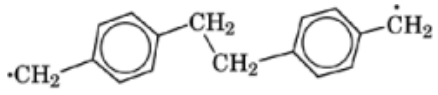

(**5**)

When the pyrolysis gases are quenched with a molar excess of iodine vapor, a yield of greater than 50% *p*-xylylene diiodide is recovered. The observation of this effect offered the first direct chemical support for the idea that DPX pyrolysis results in PX (**1**) (3).

Moreover, where *ar*-acetyldi-*p*-xylylene [10029-00-2](**6**) is pyrolyzed, by adjusting temperatures in the deposition region, it is possible to isolate two different polymeric products, ie, poly(acetyl-*p*-xylylene) [67076-72-6] (**8**) and poly(*p*-xylylene) (PPX) (**2**). This of course requires the cleavage of the original dimer into two fragments.

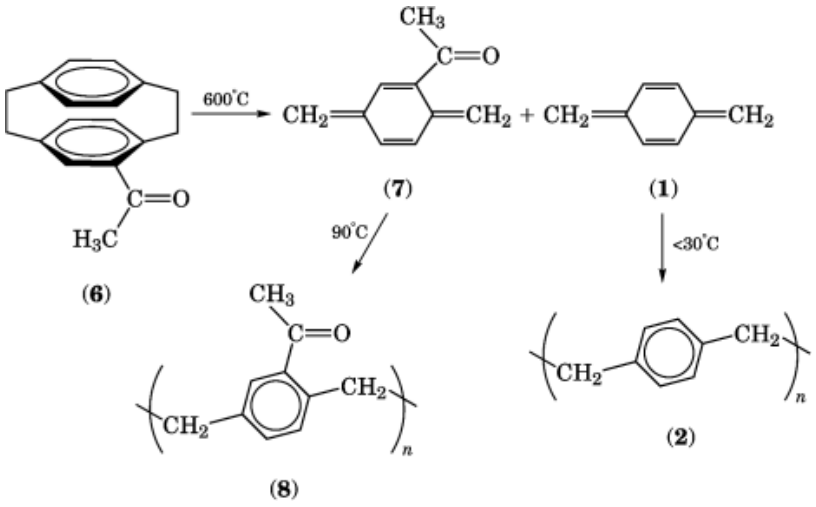

(**6**) (**7**) (**1**) (**8**) (**2**)

Experiments with monoethyl and monocarbomethoxy di-*p*-xylylene (4) gave similar results. These experiments do not, however, shed any light on whether the rupture of the methylene–methylene bonds in the dimer upon pyrolysis is simultaneous or sequential.

Only one exception to the clean production of two monomer molecules from the pyrolysis of dimer has been noted. When α-hydroxydi-*p*-xylylene (**9**) is subjected to the Gorham process, no polymer is formed, and the 16-carbon aldehyde (**10**) is the principal product in its stead, isolated in greater than 90% yield. This transformation indicates that, at least in this case, the cleavage of dimer proceeds in stepwise fashion rather than by a concerted process in which both methylene–methylene bonds are broken at the same time. This is consistent with the predictions of Woodward and Hoffmann from orbital symmetry considerations for such $[6 + 6]$ cycloreversion reactions in the ground state (5).

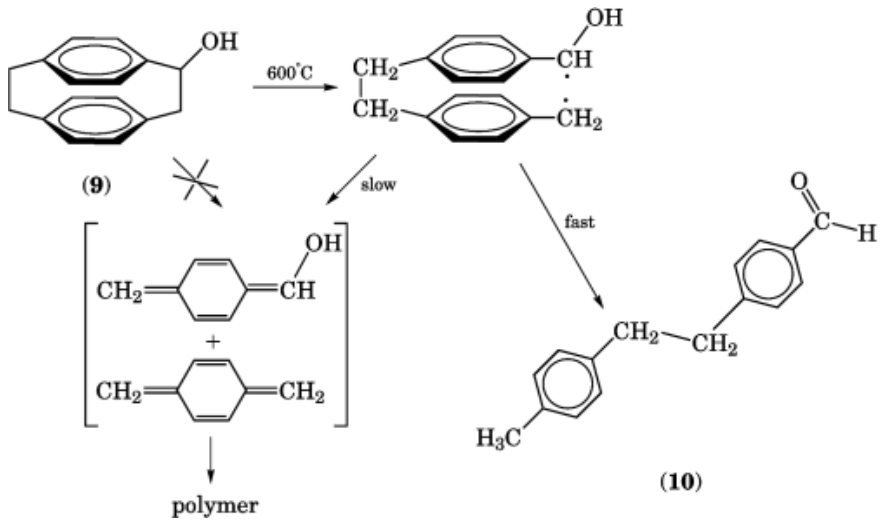

1.2. Monomer Properties

Despite difficulties involved in studying it owing to its great reactivity, a great deal is known about the structure of the parylene process monomer PX. The eight-carbon framework is planar (6). The molecule is diamagnetic, ie, all electron spins are paired in the ground state (spectroscopically, a singlet). Although many have ascribed its reactivity to its so-called biradical nature, the true biradical (triplet) form (**11**) of the molecule, an electronically excited state, is substantially more energetic, estimated at ca 50 kJ/mol (12 kcal/mol), and therefore cannot contribute to the monomer at equilibrium to any appreciable extent, even at pyrolysis temperatures. The PX molecule is instead a conjugated tetra olefin whose particular arrangement gives it extreme reactivity at its end carbons.

(**11**)

This extreme reactivity of PX has precluded many experimental approaches that otherwise would have been useful in studying it. Most of the present structural knowledge has been gleaned from spectroscopic studies and molecular orbital calculations. A noteworthy exception is an electron diffraction study (7) in which an electron beam was directed at a stream of gaseous PX, generated much as it is in the parylene process, issuing from a nozzle in a specially constructed apparatus. The results of the study are shown in Figure 2. Although the study was unable to resolve the lengths of the two different C═C and C—H bonds, it clearly distinguished between the C—C and C═C bond lengths. Thus *p*-xylylene is experimentally demonstrated to have an olefinic geometry rather than that of an aromatic biradical.

By trapping PX at liquid nitrogen temperature and transferring it to THF at $-80^{\circ}C$, the ^{1}H nmr spectrum could be observed (9). It consists of two sharp peaks of equal area at chemical shifts of 5.10 and 6.49 ppm downfield from tetramethylsilane (TMS). The fact that any sharp peaks are observed at all attests to the absence of any significant concentration of unpaired electron spins, such as those that would be contributed by the biradical (**11**). Furthermore, the chemical shift of the ring protons, 6.49 ppm, is well upfield from the typical aromatic range and more characteristic of an olefinic proton. Thus the olefin structure (**1**) for PX is also supported by nmr.

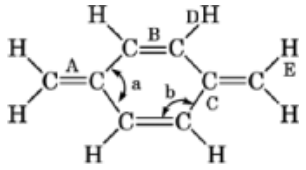

Fig. 2. Structure of PX monomer molecule from electron diffraction (8). Bond lengths: C═C, A=B+0.1381±0.008; C–C, C=0.1451±0.0007 nm; C–H, D=E=0.1116±0.0035 nm. Bond angles: a=122.2±3.7°, b=118.9±1.9°.

A particularly useful property of the PX monomer is its enthalpy of formation. Conventional means of obtaining this value, such as through its heat of combustion, are, of course, excluded by its reactivity. An experimental attempt was made to obtain this measure of chemical reactivity with the help of ion cyclotron resonance; a value of 209 ± 17 kJ/mol (50 ± 4 kcal/mol) was obtained (10). Unfortunately, the technique suffers from lack of resolution in addition to experimental imprecision. It is perhaps better to rely on molecular orbital calculations for the formation enthalpy. Using a semiempirical molecular orbital technique, which is tuned to give good values for heat of formation on experimentally accessible compounds, the heat of formation of *p*-xylylene has been computed to be 234.8 kJ/mol (56.1 kcal/mol) (11).

1.3. Successful p-Xylylene VDP Monomers

Within the limits mentioned above, it is frequently possible, and often desirable, to modify the *p*-xylylene monomer by attaching to it certain substituents. Limitations on such modifications lie in three areas: reactivity, performance in the coater, and cost.

1.3.1. Reactivity

Although the reactivity which enables the gas–solid polymerization to proceed is a characteristic of the eight-carbon *p*-xylylene tetraolefin system, it is possible to subdue that reactivity. For example, by attaching electron-withdrawing substituents to the alpha positions and thereby further delocalizing the π-electrons of the highly reactive *p*-xylylene nucleus, it is in several instances possible to prepare *p*-xylylenes that are so stable that they can be isolated and handled as normal organic compounds (Fig. 3). These sorts of substitutions must of course be avoided if the goal is to make polymer.

It is also possible to interfere with the polymerization by attaching at the alpha positions either too many groups, or groups which are too bulky. Four chlorine atoms (12) or four methyl groups (13) seem to be sufficient to hinder the production of polymer. These crowded *p*-xylylene monomers can be polymerized, but not through a VDP process.

Thus, except for electron-withdrawing or bulky substituents, at least from the standpoint of reactivity toward polymerization, modification by most other substituents is possible.

1.3.2. Performance in Coater

The modified monomer should perform well in commercial deposition equipment. Performance considerations include the growth rate of the coating, the uniformity of thickness of the coating over the chamber volume, and the efficiency with which the dimer is converted to useful coatings on the substrates.

An important further constraint is the fact that economic considerations in the construction of deposition equipment normally lead to a preference for an ambient temperature deposition chamber. Control of deposition temperature is possible, but it adds both equipment expense and operational complexity.

The vapor pressure of a parylene monomer is a prime factor in determining how rapidly a coating grows when exposed to an atmosphere of monomer at a given pressure. Vapor pressure is reduced as molecular

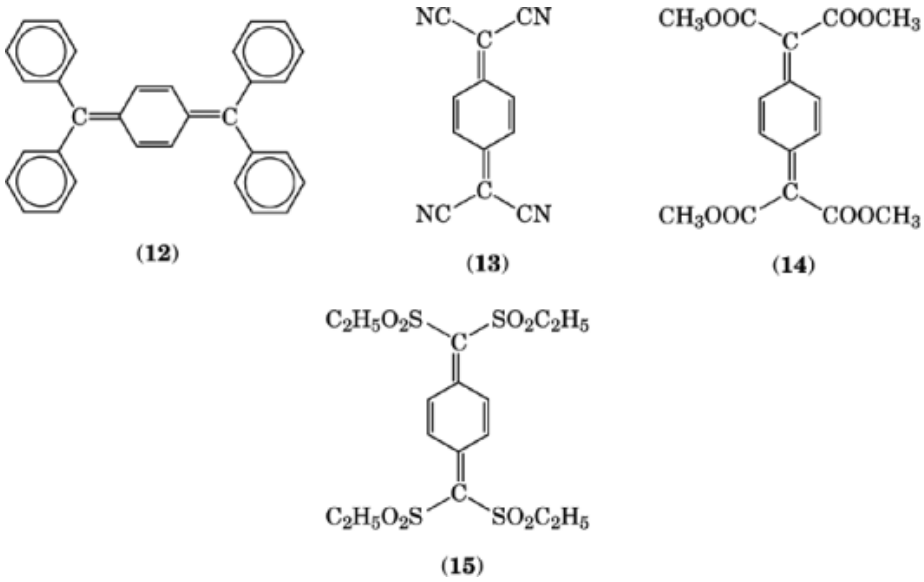

Fig. 3. Isolatable *p*-xylylene derivatives: (**12**), Thiele's hydrocarbon - 1904 [26392-12-1]; (**13**), tetracyanoquinodimethane [1518-16-7] (TCNQ); (**14**), tetrakis(methoxycarbonyl)-quinodimethan [65649-20-9]; (**15**), tetrakis(ethylsulfonyl)quinodimethan [84928-90-5].

weight increases, thereby increasing the monomer's tendency to condense and, along with it, increasing the VDP growth rate. The presence of polar functionality in the molecule further depresses vapor pressure. But too low a vapor pressure makes it difficult to transport gaseous monomer from point to point in the deposition chamber. Hence, some optimum value of monomer volatility is expected.

The widely used Parylene C owes its popularity principally to the room temperature volatility of its monomer. The Parylene C monomer, chloro-*p*-xylylene, has become the de facto performance standard. By comparison, the Parylene N monomer, *p*-xylylene itself, is too volatile and would perform better in a sub-ambient temperature deposition system. The Parylene D monomer, dichloro-*p*-xylylene [85586-88-5] is too heavy, and causes distribution problems in larger deposition systems.

1.3.3. Cost

It is necessary to produce the feedstock from which the monomer is generated, viz, the dimer, at a cost which can be supported by the commercial application, and yet allow it to be economically competitive with all other alternative ways to achieve the same end result. This factor often, but not always, seriously limits the amount of effort that can be put into dimer synthesis and purification.

2. Other, Related Processes

VDP processes using means other than the pyrolytic cleavage of DPX (Gorham process) to generate the reactive monomer are also known, although none are practiced commercially at the time of this writing (ca 1997).

2.1. Photopolymerization and Plasma Polymerization

The use of ultraviolet light alone (14) as well as the use of electrically excited plasmas or glow discharges to generate monomers capable of undergoing VDP have been explored. The products of these two processes, called plasma polymers, continue to receive considerable scientific attention. Interest in these approaches is enhanced by the fact that the feedstock material from which the monomer capable of VDP is generated is often inexpensive and readily available. In spite of these widespread scientific efforts, however, commercial use of the technologies is quite limited.

When *p*-xylene is used as the monomer feed in a plasma polymer process, PX may play an important role in the formation of the plasma polymer. The plasma polymer from *p*-xylene closely resembles the Gorham process polymer in the infrared, although its spectrum contains evidence for minor amounts of nonlinear, branched, and cross-linked chains as well. Furthermore, its solubility and low softening temperature suggest a material of very low molecular weight (15).

2.2. VDP Polyimides

Polyimide films have also been prepared by a kind of VDP (16). The poly(amic acid) layer is first formed by the coevaporation and condensation of two monomers, followed by copolymerization on the substrate. The imidization is carried out in a separate baking step (see POLYIMIDES).

2.3. o-Xylylene/BCB

Thermosetting resins based on benzocyclobutene (BCB)

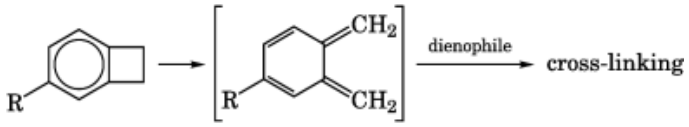

chemistry have been reported (17). In these condensed phase cures, the *ortho*-xylylene isomer is the key reactive intermediate. From the behavior of this energetically similar ortho isomer, the value of the para configuration's rendering any ring closure reaction, analogous to cyclobutene formation from the ortho isomer, geometrically forbidden can be appreciated.

3. Dimer

In contrast to the extreme reactivity of the monomeric PX (**1**) generated from it, the dimer DPX (**3**) feedstock for the parylene process is an exceptionally stable compound. Because of their chemical inertness, dimers in general do not exhibit shelf-life limitations. Although a variety of substituted dimers are known in the literature, at present only three are commercially available: DPXN, DPXC, and DPXD, which give rise to Parylene N, Parylene C, and Parylene D, respectively.

The unsubstituted C-16 hydrocarbon, [2.2]paracyclophane (**3**), is DPXN. Both DPXC and DPXD are prepared from DPXN by aromatic chlorination and differ only in the extent of chlorination; DPXC has an average of one chlorine atom per aromatic ring and DPXD has an average of two.

8 XYLYLENE POLYMERS

3.1. Manufacture

For the commercial production of DPXN (di-*p*-xylylene) (**3**), two principal synthetic routes have been used: the direct pyrolysis of *p*-xylene (**4**, $X = Y = H$) and the 1,6-Hofmann elimination of ammonium (HNR_3^+) from a quaternary ammonium hydroxide (**4**, $X = H$, $Y = NR_3^+$). Most of the routes to DPX share a common strategy: PX is generated at a controlled rate in a dilute medium, so that its conversion to dimer is favored over the conversion to polymer. The polymer by-product is of no value because it can neither be recycled nor processed into a commercially useful form. Its formation is minimized by careful attention to process engineering. The chemistry of the direct pyrolysis route is shown in equation **1**:

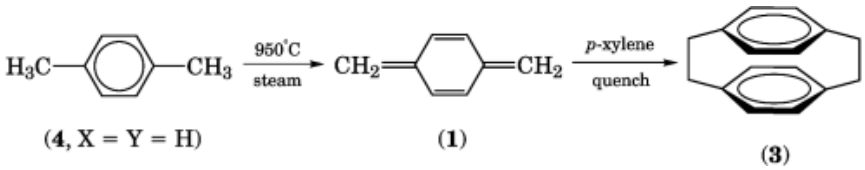

(**4**, X = Y = H) (**1**) (**3**) (1)

First, *p*-xylene is dehydrogenated pyrolytically in the presence of steam at about 950°C to give *p*-xylylene (PX), which in turn forms di-*p*-xylylene (DPX) when quenched in liquid xylene. The xylene is recycled to the pyrolysis vessel. Yields and conversion efficiency are satisfactory. However, several engineering challenges need to be overcome, including the choice of a suitable diluent; establishing optimal residence time, vapor velocity, and operating pressure during pyrolysis; and the design and construction of novel equipment to withstand the highly corrosive reaction environment.

The Hofmann elimination route, of which many versions exist, can be carried out at much lower temperatures in conventional equipment. The PX is generated by a 1,6-Hofmann elimination of amine from a quaternary ammonium hydroxide in the presence of a base. This route gives yields of 17–19%. Undesired polymeric products can be as high as 80% of the product. In the presence of a polymerization inhibitor, such as phenothiazine, DPXN yields can be increased to 50%.

In the 1,6-elimination of *p*-trimethylsilylmethylbenzyltrimethylammonium iodide with tetrabutylammonium fluoride, yields as high as 56% have been reported (18). The starting materials are not readily accessible, however, and are costly.

The yield can be raised to 28% if the Hofmann elimination is conducted in the presence of a water-soluble copper or iron compound (19). Further improvements up to 50% were reported when the elimination was carried out in the presence of ketone compounds (20). Further beneficial effects have been found with certain cosolvents, with reported yields of greater than 70% (8).

3.1.1. DPXC and DPXD

The economic pressure to control dimer costs has had an important effect on what is in use today (ca 1997). Attaching substituents to the ring positions of a [2.2]paracyclophane does not proceed with isomeric exclusivity. Indeed, isomeric purity in the dimer is not an essential requirement for the obtaining of isomeric purity, eg, monosubstituted monomer, in the pyrolysis. Any mixture of the four possible heteronuclearly disubstituted dichloro[2.2]paracyclophanes, will, after all, if pyrolyzed produce the same monomer molecule, chloro-*p*-xylylene [10366-09-3] (**16**) (Fig. 4).

Although DPXC and DPXD prepared by the chlorination of DPXN are relatively complex mixtures, after pyrolytic cleavage the resulting mixture of monomers is considerably simpler. Thus DPXC, when pyrolyzed, gives predominantly monochloro PX, which is accompanied by small but significant amounts of PX and dichloro PX. The resulting polymer, Parylene C, consequently has an average of about one chlorine atom per repeat unit. However, it contains significant amounts of unchlorinated, as well as dichlorinated, repeat units.

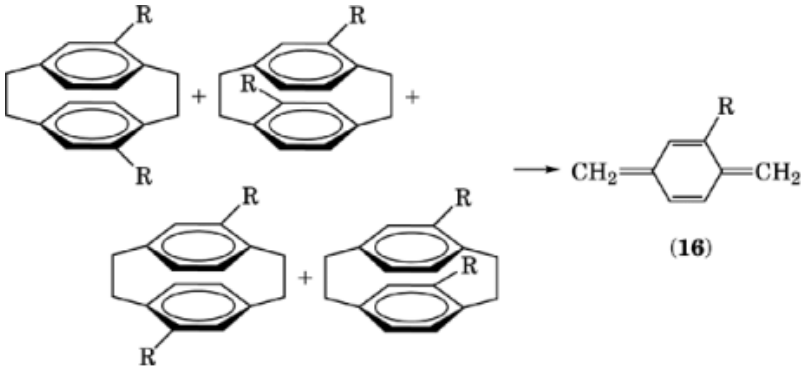

Fig. 4. Isomeric dichloro[2.2]paracyclophanes produce the same xylylene.

DPXC and DPXD are prepared from DPXN by chlorinating to different extents. The conditions are controlled to favor aromatic ring chlorination to the exclusion of the free-radical chlorination of the ethylene bridges. However, the chlorination products are complex mixtures of the homologues DPXN, monochloro DPX, dichloro DPX, trichloro DPX, and tetrachloro DPX, and even higher homologues, as well as the several possible isomers of each.

New synthetic routes for the preparation of homologously pure dichloro DPX and tetrachloro DPX have been reported through the 1,6-Hofmann elimination of chlorinated *p*-methylbenzyltrimethylammonium hydroxide. In the case of dichloro DPX, yields of 30% were reported (21). In the presence of ketone compounds, yields were increased to 50% (20).

3.2. Purification

Unsubstituted di-*p*-xylylene (DPXN) is readily purified by recrystallization from xylene. It is a colorless, highly crystalline solid. The principal impurity is polymer, which fortunately is insoluble in the recrystallization solvent and easily removed by hot filtration.

In purifying DPXC and DPXD, care must be taken not to disturb the homologue composition, so that product uniformity is maintained. For example, a recrystallization of DPXC from ethanol would give a higher melting, more crystalline dimer material, at the expense of a decrease in yield owing to the removal of otherwise useful isomers, but the polymer made from it would not be identical to the historical Parylene C, as defined by its preparation from the chlorination mixture. The real purification issues are the removal of insoluble residues and any components that contain aliphatic side-chain chlorine. Although ring-substituted chlorine is stable, side-chain chlorine can give rise to hydrogen chloride gas under the conditions of the parylene process, or subsequent to it, which in certain applications could initiate substrate corrosion. Fortunately, the aliphatic chlorine problem can be minimized by proper attention to process detail.

3.3. Properties

The DPXs are all crystalline solids; melting points and densities are given in Table 1. Their solubility in aromatic hydrocarbons is limited. At 140°C, the solubility of DPXN in xylene is only about 10%. DPXC is more readily soluble in chlorinated solvents, eg, in methylene chloride at 25°C its solubility is 10%. In contrast, the corresponding figure for DPXN is 1.5%.

The structure of DPXN was determined in 1953 from x-ray diffraction studies (22). There is considerable strain energy in the buckled aromatic rings and distorted bond angles. The strain has been experimentally

Table 1. Properties of Parylene Dimers

Dimer	Melting point, °C	Density, g/cm^3
DPXN	284[a]	1.22
DPXC	140–160[b]	1.30
DPXD	170–195[b]	1.45

[a]Decomposes.
[b]Mixture of homologues and their isomers.

quantified at 130 kJ/mol (31 kcal/mol) by careful determination of the formation enthalpy through heat of combustion measurements (23). The release of this strain energy is doubtless the principal reason for success in the particularly convenient preparation of monomer in the parylene process.

4. Polymer

The linear polymer of PX, poly(*p*-xylylene) (PPX) (**2**), is formed as a VDP coating in the parylene process. The energetics of the polymerization set it apart from all other known polymerizations and enable it to proceed as a vapor deposition polymerization.

5. Thermodynamic Considerations

On the basis of the value for the enthalpy of formation of *p*-xylylene, ΔH^0_f(PX), the enthalpy of polymerization, $\Delta H^0_{\text{polym}} = \Delta H^0_f(\text{PPX}) - \Delta H^0_f(\text{PX})$, can be estimated. No experimental combustion data are available for high molecular weight poly(*p*-xylylene) as it is formed in the parylene process, ΔH^0_f(PPX).

For crystalline [2.2]paracyclophane [(l), DPXN], a ΔH^0_f of +154.4 kJ/mol (+ 36.9 kcal/mol) is reported (23). The hypothetical transformation of crystalline DPXN into polymer is accompanied by the release of 129.7 kJ/mol (31.0 kcal/mol) of paracyclophane strain energy per mole of paracyclophane, and 12.6 kJ/mol (3.0 kcal/mol) per polymer repeat unit as a result of the bibenzyl hyperconjugative stabilization, which is permitted in the polymer but excluded by geometry in the dimer. Thus the standard enthalpy of formation for the hypothetical 100% crystalline poly(*p*-xylylene) is estimated to be −0.3 kJ/mol (− 0.05 kcal/mol), assuming that the energies associated with crystallinity are the same in both cases. Although it might be acceptable to assume that such energies per repeat unit are similar in the crystalline polymer and crystalline dimer, Parylene N, as produced by the parylene process, is typically only about 57% crystalline. Using a value of 14.1 kJ/mol (3.37 kcal/mol) for the heat of fusion for poly(*p*-xylylene) (24), the standard formation enthalpy for Parylene N, as it is typically deposited in the parylene process, ΔH^0_f(Parylene N), is +5.7 kJ/mol (+ 1.4 kcal/mol).

In estimating the enthalpy of polymerization, the physical state of both starting monomer and polymer must be specified. Changes in state are accompanied by ethalpy changes. Therefore, they also affect the level of the polymerization enthalpy. The ΔH^0_f for *p*-xylylene previously mentioned is applicable to the monomer as an ideal gas. To make comparisons with other polymerization processes, most of which start with condensed monomer, a heat of vaporization for *p*-xylylene is needed. It is assumed herein that it is the same as that for *p*-xylene, 42.4 kJ/mol (10.1 kcal/mol). Thus the ΔH^0_f of the liquid monomer *p*-xylylene is 192.3 kJ/mol (46.0 kcal/mol).

The enthalpy of polymerization of unannealed (57crystalline) Parylene N, as it is deposited, starting with liquid monomer, $\Delta H^0_{\text{polym(lu)}}$, is −186.6 kJ/mol (− 44.6 kcal/mol). This is an exceptionally high value compared with those of other addition polymers, which generally fall in the −60 to −100 kJ/mol (−14.3 to −23.8 kcal/mol) range. It quantifies the vigor of the polymerization. Because the source of polymerization

enthalpy is within the *p*-xylylene system, substituents affect it only to a minor extent. All parylenes are expected to have a similar molar enthalpy of polymerization. An experimental value for the heat of polymerization of Parylene C has appeared. Using the gas evolution from the liquid nitrogen cold trap to measure thermal input from the polymer, and taking advantage of a peculiarity of Parylene C at $-196^{\circ}C$ to polymerize abruptly, perhaps owing to the arrival of a free radical, a $\Delta H^0_{polym} = -152 \pm 8$ kJ/mol (-36.4 ± 2.0 kcal/mol) at $-196^{\circ}C$ was reported (25). The correction from $-196^{\circ}C$ to room temperature is estimated at -17 kJ/mol, bringing this experimental value for Parylene C closer to the calculated value for Parylene N. It is assumed that S_{polym} is 0 at 0 K (3rd law), 125 J/(mol·K) [30 cal/(mol·K)] at 298 K, and proportional to T in between, a crude assumption, but appropriate to the current level of knowledge. Thus experiment and calculation are in harmony in quantifying the exceptional exothermicity of parylene polymerization.

The thermodynamic ceiling temperature (26) T_c for a polymerization is computed by dividing the ΔH^0_{polym} by the standard entropy of polymerization, ΔS^0_{polym}. The T_c is the temperature at which monomer and polymer are in equilibrium in their standard states at 25°C (298.15 K) and 101.3 kPa (1 atm). (In the case of *p*-xylylene, such a state is, of course, purely hypothetical.) The T_c quantifies the binding forces between monomer units in a polymer and measures the tendency of the polymer to revert back to monomer. In other systems, the T_c indicates a temperature above which the polymer is unstable with respect to its monomer, but in the case of parylene it serves rather as a means of comparing the relative stability of the polymer with respect to its reversion to monomer. For computing the T_c, however, the standard entropies of polymerization are required.

The standard polymerization entropies can be estimated from the following. The standard entropy S^0 for PX as an ideal gas is computed by a group-contribution method (27) to be 310.6 J/(mol·K) [74.24 cal/(mol·K)]. The entropy of vaporization for PX is assumed to be the same as that of *p*-xylene, 104.7 J/(mol·K) [25.03 cal/(mol·K)] (28). Therefore, the S^0 for liquid PX is 205.9 J/(mol·K) [49.21 cal/(mol·K)]. Noting that the experimental specific heat C_p of PPX follows that of polystyrene over the range of 160 to 340 K (29), it can be assumed that the proportionality continues down to 0 K and that the factor 135/116 at 298 K can be applied to the known S^0 for polystyrene [$S = 128.5$ J/(mol·K) or 30.70 cal/(mol·K)] (30). It follows that the S^0 for as-deposited 57%crystalline Parylene N is 149.5 J/(mol·K) [35.73 cal/(mol·K)]. Therefore, $\Delta S^0_{polym(g)} = -161.1$ J/(mol·K) [-38.50 cal/(mol·K)] and $\Delta S^0_{polym(l)} = -56.4$ J/(mol·K) [-13.48 cal/(mol·K)].

The results of the above polymerization thermodynamics calculations for parylene are compared to similar data for typical addition polymers in Table 2. The T_c quantifies the stability of the polymer only with respect to reversion to monomer. When PPX is thermally degraded (ca 500°C), a mixture of degradation products including hydrogen gas, *p*-xylene, toluene, and *p*-methylstyrene is observed (31), suggesting that the path taken in thermal degradation requires the cleavage of bonds other than those formed in the polymerization, very likely starting with the methylene C—H bond. Complete replacement of the methylene hydrogens in PPX with fluorine gives a polymer with substantially better stability at elevated temperatures (32).

The enthalpy liberated on the VDP of parylene is real and in an adiabatic situation causes a rise in temperature of the coated substrate. For Parylene C, 229.1 kJ/mol (54.7 cal/mol) corresponds to 1654 J/g (395 cal/g) whereas its specific heat at 25°C is only 1.00 J/(g·K) [0.239 cal/(g·K)] (33). In most practical situations, however, the mass of parylene deposited is dwarfed by the substrate mass, and the heat of polymerization is dissipated within the coated substrate over the time required to deposit the coating with minimal actual temperature rise.

5.1. Polymerization Mechanism

The physical processes of condensation and diffusion must be considered along with the *p*-xylylene polymerization chemistry for a proper understanding of what happens microscopically during vapor deposition polymerization (34). These processes point to an important distinction between VDP and vacuum metallization, ie, that in the latter, adsorption is followed by a surface reorganization of the existing deposited material,

Table 2. Entropies, Enthalpies, and Ceiling Temperatures for the Polymerization of Various Monomers at 25°C (298.15 K) and 101.3 kPa (1 atm)[a]

	Liquid			Gas		
Monomer	$-\Delta H^0$, kJ/mol[b]	$-\Delta S^0$, J/(mol·K)[b]	T_c, °C	$-\Delta H^0$, kJ/mol[b]	$-\Delta S^0$, J/(mol·K)[b]	T_c, °C
ethylene	108.4	173.6	351			
propylene	81.6	116.3	429			
isoprene	74.9	101.3	467	101.3	187.0	268
styrene	69.9	104.6	395	113.4	212.1	262
methyl meth-acrylate	55.2	117.2	198			
α-methylstyrene	35.1	103.8	65			
p-xylylene	186.6	56.4	3035	229.1	161.1	1149

[a] Ref. 26.
[b] To convert J to cal, divide by 4.184.

and diffusion of incoming species through the bulk is nonexistent. In most parylene depositions, a coating forms from gaseous monomer under steady-state conditions.

Gaseous monomer is transported to the location within the coating where it is to be consumed to produce polymer by an initial condensation, followed by diffusion. The net flux of monomer molecules through the growth interface, ie, the outer boundary of the coating, between the gaseous and condensed phases, needed to sustain growth at a given rate can be readily calculated [for Parylene C, 10 μm/h requires $1.55 \times 10^{15}/(\text{cm}^2 \cdot \text{s})$]. Comparing a net flux so obtained with the flux of molecules that according to the kinetic theory of gases are striking the growth surface [$Z = PN_0/\sqrt{2\pi MRT}$] for the conditions typical of parylene deposition, a large difference (two or three orders of magnitude) is observed. For Parylene C monomer at a pressure of 1.3 Pa (10 μm Hg) and 25°C, $Z = 6.7 \times 10^{17}/(\text{cm}^2 \cdot \text{s})$. For each molecule that eventually enters the coating, some hundred or thousand molecules strike the growth interface. Those that condense and do not react must, of course, evaporate. The term "sticking coefficient" has sometimes been borrowed from vacuum metallization to describe this ratio of incident molecules to consumed molecules. However, the VDP situation is not adequately described by hard spheres bouncing off a growth interface. Every incident molecule spends at least some time in the polymeric coating phase beyond the growth interface before it is lost again to the gas phase.

Because most of the condensing molecules evaporate, condensation equilibrium at the growth surface can be assumed, to a good approximation. The concentration of monomer dissolved in the coating near the growth interface is, therefore, governed by Henry's law, and monomer concentration in polymer solution increases proportionately to the partial pressure of monomer in the gas phase. Furthermore, as the temperature is lowered, or as higher molecular weight monomers of lower volatility are selected, monomer concentration at the growth interface increases. In most practical situations, these Henry's law effects dominate in determining growth rates for VDP coatings by regulating monomer concentration within the coating. For each monomer, there exists a threshold condensation temperature, T_{tc}, above which the rate of growth of coating is, for all practical purposes, zero (Table 3), but this phenomenon is governed by the competition between initiation and propagation chemistries, discussed herein.

Once it is in "solution" in the coating, the monomer moves about in random directions by diffusion until it evaporates or is consumed by chemical reaction. The polymer molecules that have already grown to higher molecular weight cannot relocate appreciably owing to entanglement with their neighbors. The rate of diffusion of monomer through the polymer bulk is adequate for the participation of diffusive transport in the mechanism of VDP (ca 10^{-10} cm^2/s at room temperature). This can be confirmed in swelling-rate experiments with solvents having similar physical properties, such as *p*-xylene.

Table 3. Threshold Condensation Temperatures T_{tc} for Substituted p-Xylylene Monomers

Monomer	T_{tc}, °C
p-xylylene	30
2-methyl-*p*-xylylene	60
2-ethyl-*p*-xylylene	90
2-chloro-*p*-xylylene	90
2-acetyl-*p*-xylylene	130
2-cyano-*p*-xylylene	130
2-bromo-*p*-xylylene	130
dichloro-*p*-xylylene	130

The monomer is consumed by two chemical reactions: initiation, in which new polymer molecules are generated, and propagation, in which existing polymer molecules are extended to higher molecular weight. In steady-state VDP, both reactions proceed continuously inside polymeric coating, in the reaction zone just behind the growth interface.

The first step of the initiation reaction is the coupling of two monomer molecules to form the dimer diradical (**5**). The formation of this diradical is energetically uphill, ie, the energy of two benzyl radicals is greater than that of two starting *p*-xylylene systems. The rate of destruction greatly exceeds the rate of formation. Only a trace concentration of the dimer diradical species exists at equilibrium. Further reaction of the dimer diradical with monomer gives more stable diradicals. In these subsequent transformations, a *p*-xylylene is converted into a benzene with a net stabilizing effect. At some stage of oligomerization, the resulting *n*-mer diradical becomes more stable than the *n p*-xylylene molecules from which it was constructed. At this point, the new polymer molecule is formed. Thus the overall order of the initiation reaction, the reaction in which new polymer molecules are generated, is some $n > 2$. Initiation chemistry requires no species other than monomer, another unusual aspect of the polymerization chemistry of *p*-xylylene.

The order *n* of the initiation reaction has an important influence on the manner in which the VDP occurs. Because monomer molecules, even in solution at low concentration, are closer together in the condensed phase than they are in the gaseous phase, the rate of initiation is greater in the condensed phase than in the gaseous phase. The higher the order *n*, the more the condensed phase is favored. The order *n*, according to the mathematical model (34) of *p*-xylylene VDP, at the same time governs the effect of monomer pressure on growth rate at a given deposition temperature. The model predicts that growth rate should vary with the pressure raised to the power $((n + 3)/4$. Thus, if $n = 3$, the growth rate should be proportional to $p^{1.5}$. In an early attempt to determine the pressure dependence of parylene growth rate γ, an expression of $\gamma = k{\cdot}p^2$ was reported (35). A pressure exponent of 2 would be interpreted as an initiation order of $n = 5$. Although such a high order would favorably deemphasize "snow," consideration of the energetics of oligomeric *p*-xylylene diradicals would seem to place the order nearer to 3. Perhaps the early investigators did not anticipate a nonintegral order for pressure dependence. A more recent report (36) places *n* at 3 for Parylenes N and C, and 4 for Parylene D. Thus, with $n \geq 3$, the parylenes are more likely to form a continuous coating than a dust or a snow, the physical form of the product of a gas-phase polymerization. To the extent that snow is included in the formation of a coating (ie, dual-phase polymerization), haze develops.

In the propagation reaction, the monomer molecule reacts with an existing free-radical polymer chain end to make the chain one repeat unit longer. The polymer chains have two active ends, and they grow from both ends at the same time. Under normal coating conditions, the consumption of monomer by propagation must be much higher than its consumption by initiation to obtain high molecular weight polymer. In fact, the number-average molecular weight is determined by the proportion of monomer consumed by the two reactions, and is diminished by increases in deposition temperature or monomer partial pressure.

The concentration of monomer within the coating decreases approximately exponentially with distance from the growth interface. With this decrease in monomer concentration, the rates of initiation and propagation reactions also decrease. Moving back into the polymer from the growth interface, through the reaction zone where polymer is being manufactured, a region in which the polymer formation is essentially complete is gradually entered. Because initiation is of higher order in monomer concentration, it tends to occur closer to the growth interface than does propagation. Under conditions prevailing during a typical deposition, the characteristic depth of the reaction zone is a few hundred nanometers, and the maximum concentration of monomer, ie, the concentration at the growth interface, is of the order of a few tenths percent by weight. Thus the parylene polymerization takes place just behind the growth interface in a medium that is best described as a slightly swollen, solid polymer.

During the vapor deposition process, the polymer chain ends remain truly alive, ceasing to grow only when they are so far from the growth interface that fresh monomer can no longer reach them. No specific termination chemistry is needed, although subsequent to the deposition, reaction with atmospheric oxygen, as well as other chemical conversions that alter the nature of the free-radical chain ends, is clearly supported experimentally.

5.2. Polymer Properties

The single most important feature of the parylenes, that feature which dominates the decision for their use in any specific situation, is the vapor deposition polymerization (VDP) process by which they are applied. VDP provides the room temperature coating process and produces the films of uniform thickness, having excellent thickness control, conformality, and purity. The engineering properties of commercial parylenes once they have been formed are given in Table 4. As crystalline polymers, the parylenes retain useful physical integrity up to temperatures approaching their crystalline melting points. However, their glass-transition temperatures, T_g, the temperature spans over which the continuous amorphous phase, usually the minority phase, changes from a rigid, vitreous condition to a more flexible, rubbery condition, are probably in the vicinity of ambient temperature. In the case of PPX (Parylene N), careful measurements have established the T_g to be centered at 13°C, the range over which T affects heat capacity measurements extending from 240 to 330 K (-33 to +57°C) (24). Because they have similar backbone structures, other parylenes are expected to have similar T_gs, although no measurements taken with equal care exist. Earlier reports have quoted a somewhat higher (60–90°C) range for the entire family (4). In either case, the parylenes as prepared by their VDP process are further distinguished from conventional polymers in having been generated in a medium that is at least to some extent vitreous.

During formation, the motions of the parylene polymer chains in the vitreous medium are restricted. The properties of freshly deposited parylenes, therefore, generally differ from those that have been aged or annealed. Restricted polymer chain motion during VDP severely limits their ability to organize into crystallites, and consequently freshly deposited parylenes are metastable. With the passage of time, and sooner if heated, they will reorganize into a thermodynamically more satisfactory configuration, increasing crystallinity. Certain physical properties of freshly deposited parylenes therefore can be expected to change upon aging or annealing. Of the commercial materials, Parylene C, perhaps as a result of the asymmetry of its repeat unit, is particularly subject to modifications subsequent to its initial formation.

5.2.1. Mechanical Properties

Many of the mechanical properties of the parylenes are similar to those of other conventional plastics. The values in Table 4 are typical of those quoted for the parylenes, but in any particular case can vary with aging or annealing. In an outstanding instance of this effect, the 200% elongation quoted for Parylene C is the value commonly observed on the freshly deposited material. It drops dramatically as crystallinity builds. In general, an increase in crystallinity with aging or annealing results in a lowering of elongation to break and an increase

Table 4. Typical Engineering Properties of Commercial Parylenes

Property	Parylene N	Parylene C	Parylene D	ASTM method
	General			
density, g/cm^3	1.110	1.289	1.418	D1505
refractive index, n_D^{23}	1.661	1.639	1.669	
	Mechanical			
tensile modulus, GPa[a]	2.4	3.2	2.8	D882
tensile strength, MPa[b]	45	70	75	D882
yield strength, MPa[b]	42	55	60	D882
elongation to break, %	30	200	10	D882
yield elongation, %	2.5	2.9	3	D882
Rockwell hardness	R85	R80		D785
coefficient of friction				D1894
static	0.25	0.29	0.35	
dynamic	0.25	0.29	0.31	
	Thermal			
melting point, °C	420	290	380	
linear coefficient of expansion at 25°C × 10^5, K^{-1}	6.9	3.5		
heat capacity at 25°C, J/(g·K)[c]	1.3[d]	1.0[e]		
thermal conductivity at 25°C, W/(m·K)	0.12	0.082		
	Electrical			
dielectric constant				D150
60 Hz	2.65	3.15	2.84	
1 kHz	2.65	3.10	2.82	
1 MHz	2.65	2.95	2.80	
dissipation factor				D150
60 Hz	0.0002	0.020	0.004	
1 kHz	0.0002	0.019	0.003	
1 MHz	0.0006	0.013	0.002	
dielectric strength at 25 μm, MV/m				D149
short time	275	220	215	
step-by-step	235	185		
volume resistivity at 23°C, 50% RH, Ω	1.4×10^{17}	8.8×10^{16}	2×10^{16}	D257
surface resistivity at 23°C, 50% RH, Ω	1×10^{13}	1×10^{14}	5×10^{16}	D257
	Barrier			
water absorption, %	<0.1	<0.1	<0.1	D570
water vapor transmission at 37°C, ng/(Pa·s·m)[f]	0.0012	0.0004	0.0002	E96
gas permeability at 25°C, amol/(Pa·s·m)[g]				D1434
N_2	15.4	2.0	9.0	
O_2	78.4	14.4	64.0	
CO_2	429	15.4	26.0	
H_2S	1590	26.0	2.9	
SO_2	3790	22.0	9.53	
Cl_2	148	0.7	1.1	

[a]To convert GPa to psi, multiply by 145,000.
[b]To convert MPa to psi, multiply by 145.
[c]To convert J to cal, divide by 4.184.
[d]Refs. 22 and 27.
[e]Ref. 31.
[f]To convert ng/(Pa·s·m) to g-mil/(100 in^2-day) at 90% RH, 37°C, multiply by 1240.
[g]To convert amol/(Pa·s·m) to cm^3 (STP)-mil/(100 in^2-day-atm), multiply by 0.498.

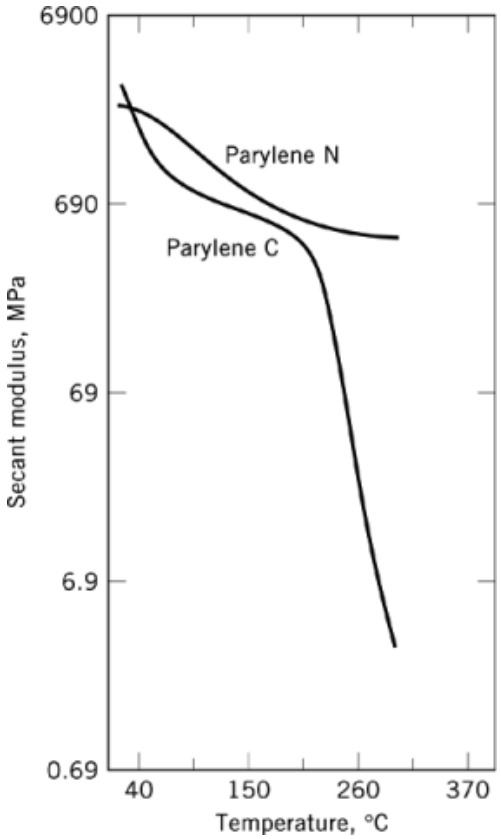

Fig. 5. Stiffness–temperature behavior of Parylenes N and C. To convert MPa to psi, multiply by 145.

in modulus and strength. The variation in mechanical rigidity of the parylenes as temperature increases is shown in Figure 5, which plots the logarithm of the secant modulus, a measure of stiffness, vs temperature. Generally, a small decrease in rigidity occurs near ambient temperature as the glass transition is traversed. Significant rigidity is then retained up to the point where the crystallites begin to melt.

It has been reported that Parylene N is deposited in a state of compressive stress (37). The inherent stress is 18 MPa (2300 psi) and is invariant with thickness. This congenital compressive stress can be removed and rendered tensile by a thermal cycle.

5.2.2. Electrical Properties

The bulk electrical properties of the parylenes make them excellent candidates for use in electronic construction. The dielectric constants and dielectric losses are low and unaffected by absorption of atmospheric water. The dielectric strength is quoted for specimens of 25 μm thickness because substantially thicker specimens cannot be prepared by VDP. If the value appears to be high in comparison with other materials, however, it should be noted that the usual thickness for such a measurement is 3.18 mm. Dielectric strength declines with the square root of increasing thickness. Viewed in this light, the dielectric strength of the parylenes is good, but not outstandingly high. The bulk resistivities are advantageously high because of the purity of the parylenes, their low moisture absorption, and in particular their freedom from the trace ionic impurities present in conventional polymers as residues. Such impurities might be the residues of the catalysts necessary for their formation. The

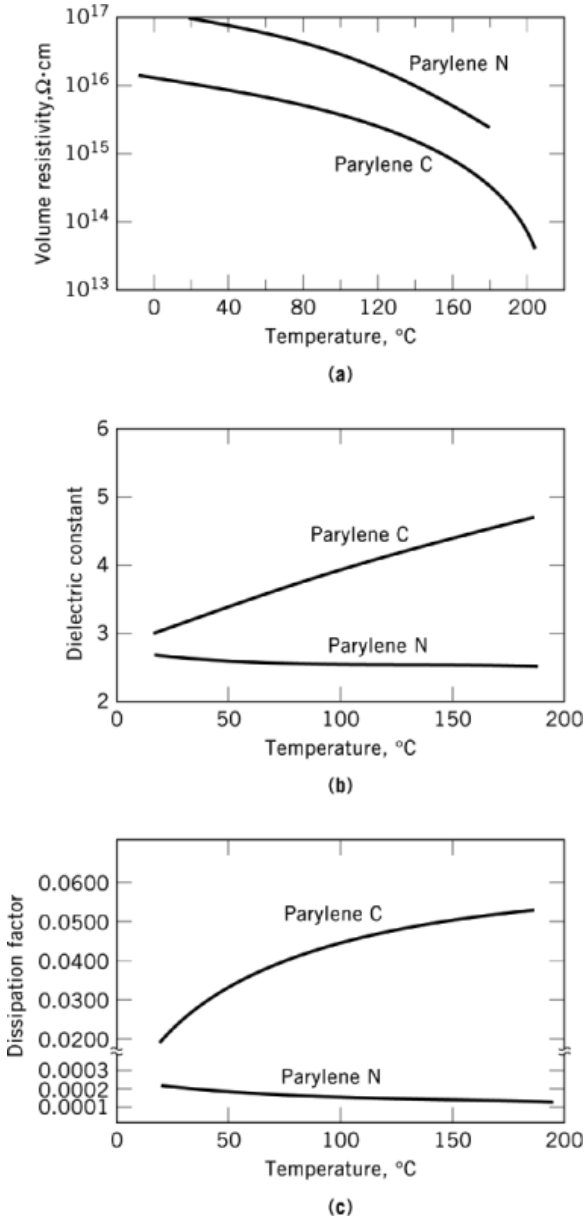

Fig. 6. Variation of electrical properties of Parylenes N and C with temperature.

surface resistivities are advantageously high in part because of their low affinity for atmospheric water. The experimental dependence of the electrical properties on temperature is shown in Figure 6.

The question of the value of the dielectric constant of the parylenes in the gigahertz range of frequencies is often of interest to designers of high frequency circuitry. Making such measurements on low loss, low dielectric constant, thin films is experimentally difficult, and no reliable data exist as of this writing (ca 1997). Fortunately, however, an indicator is available. For nonabsorbing, nonmagnetic materials such as the parylenes, the well-

Table 5. Dielectric Constants and Refractive Indexes of Parylenes

Parameter	Parylene N	Parylene C	Parylene D
dielectric constant			
60 Hz	2.65	3.15	2.84
1 kHz	2.65	3.10	2.84
1 MHz	2.65	2.95	2.80
refractive index			
n_D line	1.661	1.639	1.669
squared	2.76	2.69	2.79

known Maxwell relation applies: at any particular frequency, the square of the index of refraction equals the relative permittivity, or dielectric constant (38). The refractive indices for the parylenes at the sodium D line (589 nm), a visible wavelength that corresponds to a frequency of 510 THz ($5.10.167 >$ Hz), are shown in Table 5, along with their squares and the lower frequency measurement of dielectric constant. Because by virtue of the Maxwell relation the dielectric constants of the parylenes at the much higher frequency of visible light are close to those observed by conventional means, it seems likely that when reliable gigahertz dielectric constant measurements on the parylenes become available, similar values will be obtained.

5.2.3. Thermal Properties and Endurance

The heat capacity or specific heat, C_p is a quantity of theoretical thermodynamic significance as well as of practical importance. It has been determined for Parylene N over the temperature range of 220 to 620 K (-53 to $+347^\circ$C) (24, 29).

Figure 7 gives the results of an experiment in which freestanding films were exposed to constant elevated temperatures in air-circulating ovens for periods of weeks to months; the failure criterion was a 50% loss in tensile strength. Because the test is destructive, each data point (failure time at a given temperature) required many specimens. In the degradation of many polymers, including the parylenes, tensile strength is maintained until chain scission has reduced molecular weight to the point at which entanglement is no longer a factor in determining physical properties. Beyond that point it drops abruptly. Thus despite the relatively large variance in tensile strength measurements, the 50% loss criterion allows a reasonably precise location of end of useful life on a log time scale (Fig. 8). The data of Figure 7 suggest that Parylenes N, C, and D perform in air without significant loss of physical properties for 10 yr at 60, 80 and 100°C, respectively. Clearly, these data can justifiably be made to serve only as a guide for considering the parylenes for a specific application. Questions of thermal endurance tend to have no clear-cut answers. In situations where performance may be marginal, there is no substitute for retesting under conditions more directly relatable to the application.

5.2.4. Degradation

The most important mode of degradation for parylenes is oxidative chain scission. Significantly, hydrolytic degradation is chemically impossible. Oxidative degradation limits the use of parylenes at elevated temperatures in many common applications. Figure 9 shows the effect of exposure to elevated temperature in air or in vacuum on elongation to break, an indicator of toughness or lack of brittleness. The data are given for Parylene C, which suffers substantial change in mechanical properties as the freshly deposited material is annealed. Aging in air at 150°C for ca 100 h causes the elongation to break to drop from its initially very high value to 0, at which point the specimen is mechanically useless. Aging in vacuum at yet higher temperatures (265°C) for a similar length of time gives a stronger, more rigid, stabilized material with 15% elongation at break, the result of annealing.

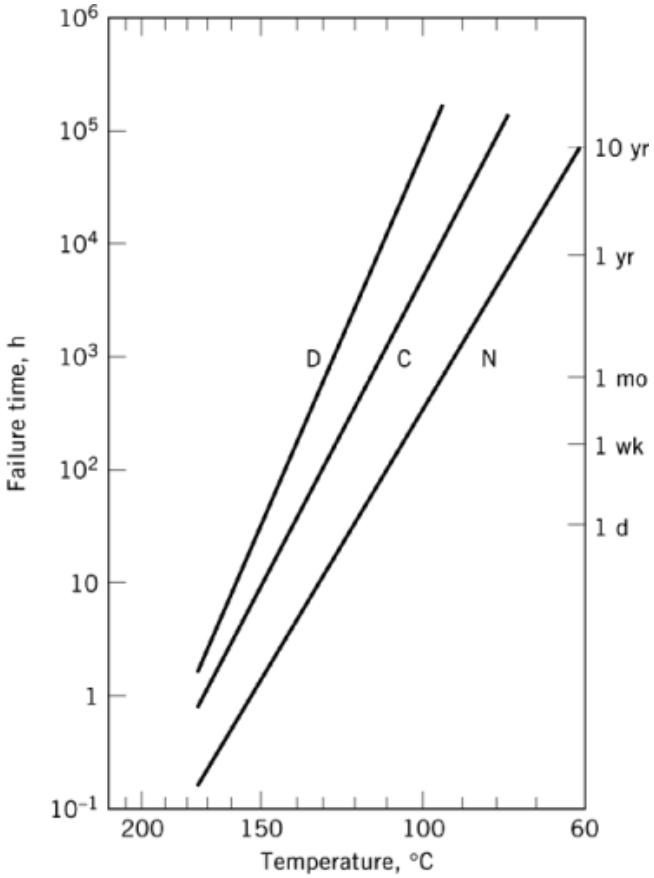

Fig. 7. Useful lifetime of Parylenes N, C, and D as a function of temperature in air. $_{\text{Failure=50\%}}$ loss in tensile strength.

For applications where oxygen can be excluded, eg, in outer space, Figure 10 shows that 10-yr use projections exceed 200°C for Parylenes N, C, and D. Conventional antioxidants, incorporated during or after VDP, can extend the life of the parylenes at elevated temperatures (39).

Another factor in oxidative degradation is ultraviolet radiation, of which sunlight is a rich source. The oxidation of parylene appears to be enhanced by ultraviolet radiation. Ozone may play a mechanistic role in the ambient temperature exposure of parylenes to ultraviolet radiation in the presence of oxygen. For the best physical endurance, exposure of the parylenes to ultraviolet light must be minimized.

5.2.5. Barrier Properties

The bulk barrier properties of parylenes are among the best of organic polymeric coatings. The data in Table 4 are the results of tests conducted some time ago, and certain entries seem unaccountably high, particularly the values for the permeability of Parylene N by SO_2 and H_2S. Because film damage might have been the cause of these high test values, experimental confirmation is advisable. More recent values for water transport rates in Parylene C films are available over the temperature range of 20–55°C in a comparative study which includes Mylar A and Kapton H (40). Similar information is provided for Parylene D in a study over the temperature range of 30–80°C (41).

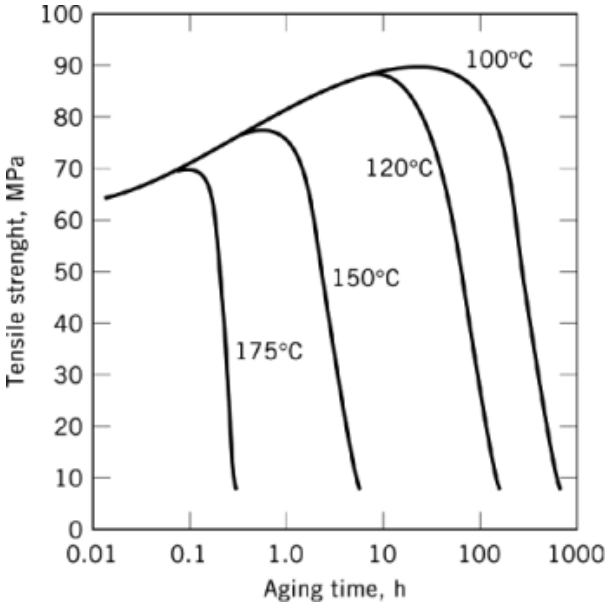

Fig. 8. Tensile strength of Parylene C on aging at elevated temperature. To convert Pa to psi, multiply by 0.145×10^{3}.

5.2.6. Spectral and Optical Properties

The parylenes do not absorb visible light, and absorb only at the shorter wavelength, high energy end of the ultraviolet range (Fig. 11). Such absorption is expected for the electronic system of the parylenes' benzene ring. Films and coatings are colorless in the visible, becoming opaque to sufficiently short wavelength uv light.

The infrared transmission spectra of Parylenes N, C, and D are compared in Figure 12. Infrared spectra can be used to distinguish among sample films of the three commercial materials should a practical question of identity arise. The spectra in Figure 12 are taken on films of ca 18-μm thickness, which gives a good picture of a typical organic film in the standard infrared presentation format. It is, however, thicker than normally encountered in a typical parylene application. The amount of incident light absorbed at any given wavelength is predictably less than that indicated by the ordinate of Figure 12.

Interference effects, which arise because of the extraordinary uniformity of thickness of the film over the spectrometer sample beam, superimposed on the absorption of incident light by parylene films, can be observed. Experimentally, a sinusoidal undulation of the baseline of the spectrum is seen, particularly in the spectral regions where there is little absorption by the sample. These so-called "interference fringe" excursions can amount to some 15–20% transmission and are uniformly spaced in frequency. Larger excursions indicate greater uniformity in thickness. Such fringes are seen toward the left side of the experimental spectra of Figure 12. Although interference phenomena are also encountered experimentally in the visible and ultraviolet regions, their effects have been removed in the consolidation and replotting of the data of Figure 11. In transmission spectra, at the top of the interference fringes (the wavelengths of the sinusoidal maxima), constructive interference occurs in which all incident light that is not absorbed appears for detection. At the fringe troughs (the wavelengths of the sinusoidal minima), a condition of destructive interference exists, at which a portion of the incident beam is reflected back toward the source, thereby escaping detection even though it is not absorbed by the sample. By observing the wavelengths at which constructive interference occurs, the

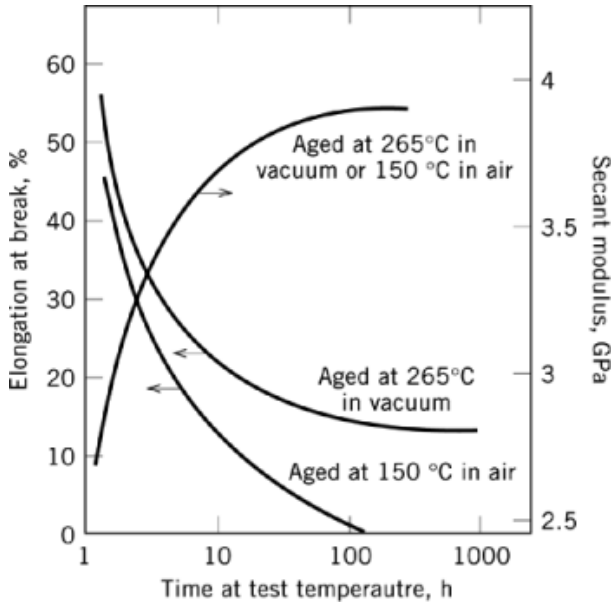

Fig. 9. Effect of temperature on the flexibility of Parylene C in air and vacuum. To convert GPa to psi, multiply by 145,000.

approximate thickness of the sample can be determined by using the expression

$$d = \frac{m\lambda_1\lambda_2}{2\,R(\lambda_1 - \lambda_2)}$$

where λ_1 and λ_2 are any two wavelengths at which interference transmission maxima (ie, constructive fringes) exist, separated by m-1 intervening constructive fringes; R is the refractive index of the sample film. The thickness d takes the units of wavelength used for λ. At any condition of constructive interference (fringe), twice the thickness times the refractive index equals an integral number of wavelengths of the incident light. That integer is known as the order of the fringe. Much more precise and accurate thicknesses may be computed from the experimental optical spectra if the order of the fringe is known and if any variation of refractive index with wavelength is taken into consideration.

Unstretched PPX films exhibit an inherent negative birefringence, the optical axis of which is perpendicular to the plane of the film. The refractive index along the optical axis is lower than the refractive index observed in the plane of the film, the difference being $n_e - n_0 = -0.075 \pm 0.001$ (42). Where they are observed from the direction normal to the film plane, the films appear to be isotropic. Birefringence is observable only when the films are tilted, or observed in cross section. When stretched, PPX films exhibit a much greater birefringence. The stretch birefringence has an optical axis in the direction of stretch and is positive: $n_z - n_0 = +0.2$.

5.2.7. Surface Energy

The surface energies of Parylenes N, C, and D were measured by observing the contact angles for several standard probe liquids. All three have surface energies of approximately 45 mJ/m^2 (= dyn/cm), ie, all test liquids having less than 45 mJ/m^2 surface tension completely wet the as-deposited parylene surfaces (43).

Plasma treatments using reactive gases (N_2, O_2) as well as inert gases (Ar, He) seemed universally to lower the contact angle for water, an observation that would imply that all such treatments raise the surface energy. Reflectance spectroscopy confirmed the presence of carbonyl in all plasma-treated specimens. Surprisingly, the

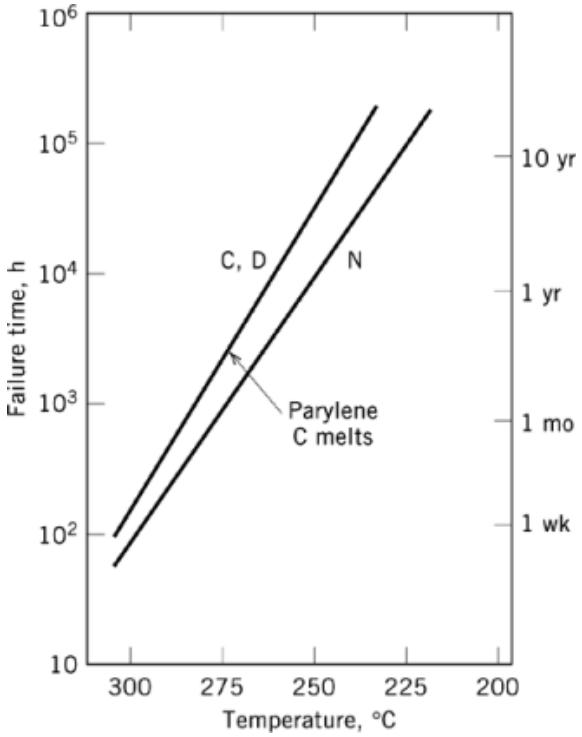

Fig. 10. Long-term effect of aging in vacuum on flexibility of Parylenes C, D, and N at elevated temperature. Failure=50% loss in tensile strength.

inert-gas-plasma treatments affected the surface energies of the parylenes more than the reactive gas plasmas did, as indicated by a water contact angle. However, the surface energies of the plasma-treated specimens universally dropped toward the original value on standing in air, but stabilized in about 1 d without recovering the original value. Plasma treatment of parylene surfaces markedly improves the adhesion of polyurethanes, a result that could be in part, at least, the result of the surface energy change.

5.2.8. Crystallinity

The crystallinity of the parylenes determines two of their most important practical characteristics: mechanical strength at elevated temperatures (see Fig. 5) and solvent resistance.

In a manner typical of crystalline polymers, the crystallinity of parylenes is confined to small-submicrometer domains that are randomly dispersed throughout an amorphous continuum. Adjacent polymer chains, in order to acquire greater overall system stability, exhibit a preference to be close to one another, but the extent to which they actually can be is limited by the tangles already present. Because a given polymer chain is long enough to participate successively in several crystallites, these crystallites function as cross-links to strengthen the bulk polymer. This structural role of the crystallites is retained as temperature rises, giving the bulk polymer physical strength even above its glass-transition temperature, where the amorphous phase is changed to a low modulus, rubbery consistency. Because the crystalline domains are much more resistant to permeation than the amorphous phase, they retain their reinforcing structural role even in the presence of permeants in the amorphous phase, thus giving the parylenes their resistance to solvent attack. The crystalline content increases in freshly deposited polymer as it ages, particularly when it is heated.

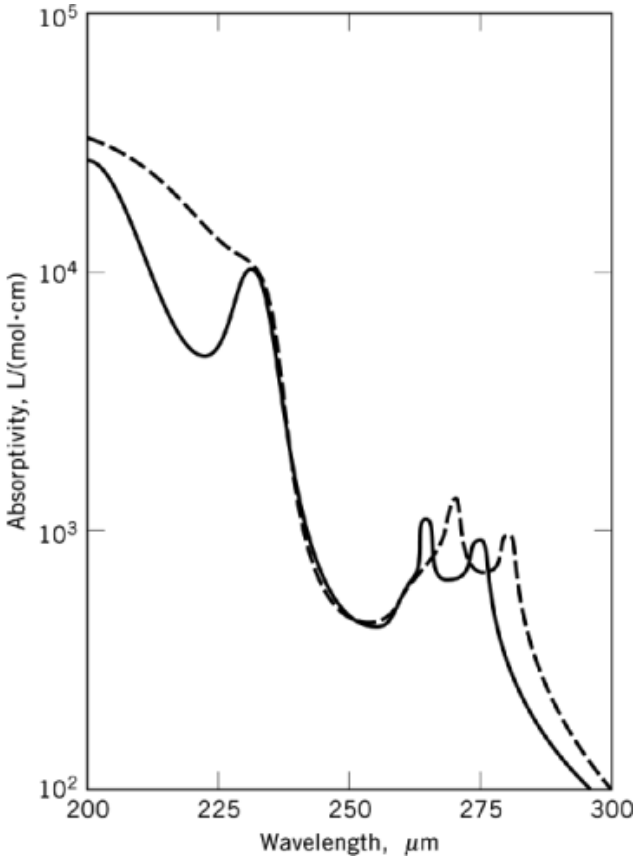

Fig. 11. Ultraviolet absorption spectra of Parylenes N (—) and C (— — —).

Parylene N (PPX) possesses a singularly complex crystalline morphology in which two distinct crystalline modifications are recognized. When deposited in the usual VDP fashion, the crystallites tend to be mostly of the α modification. On annealing at a temperature of about 220°C, the α form is converted to the β modification. This transition was originally thought to be irreversible, but studies have demonstrated that it can be made reversible (44). The crystalline phase undergoes further modifications at higher temperatures before reaching its melting point of 420°C; these modifications have not been fully explored. The detailed crystal structures of the α (a = 592 pm, b = 1060 pm, c = 655 pm, β = 134.7°, for two monomer repeat units per cell) (45) and β ($a = b$ = 2052 pm, c = 655 pm, γ = 120°, for 16 monomer repeat units per cell) (46) modifications have been determined.

In Parylene C, the single crystalline form observed is very similar to the α form of Parylene N. Its detailed crystal structure has been determined (a = 596 pm, b = 1269 pm, c (chain axis) = 666 pm, β = 135.2°) (47). X-ray studies on the crystal structure of Parylene D have not been reported.

The diffraction pattern produced where x-rays or electrons are directed perpendicularly at the film is the familiar pattern of concentric rings (a powder pattern) produced where the crystallites within the sample are randomly oriented. When the incident beam is directed at an angle to the plane, however, the uniform rings break up into bands or spots, indicative of a preferred orientation of unit cells. Tilted electron diffraction results (48) demonstrate that in Parylene N there is a preference for the ⟨100⟩ face of the unit cell to lie in the

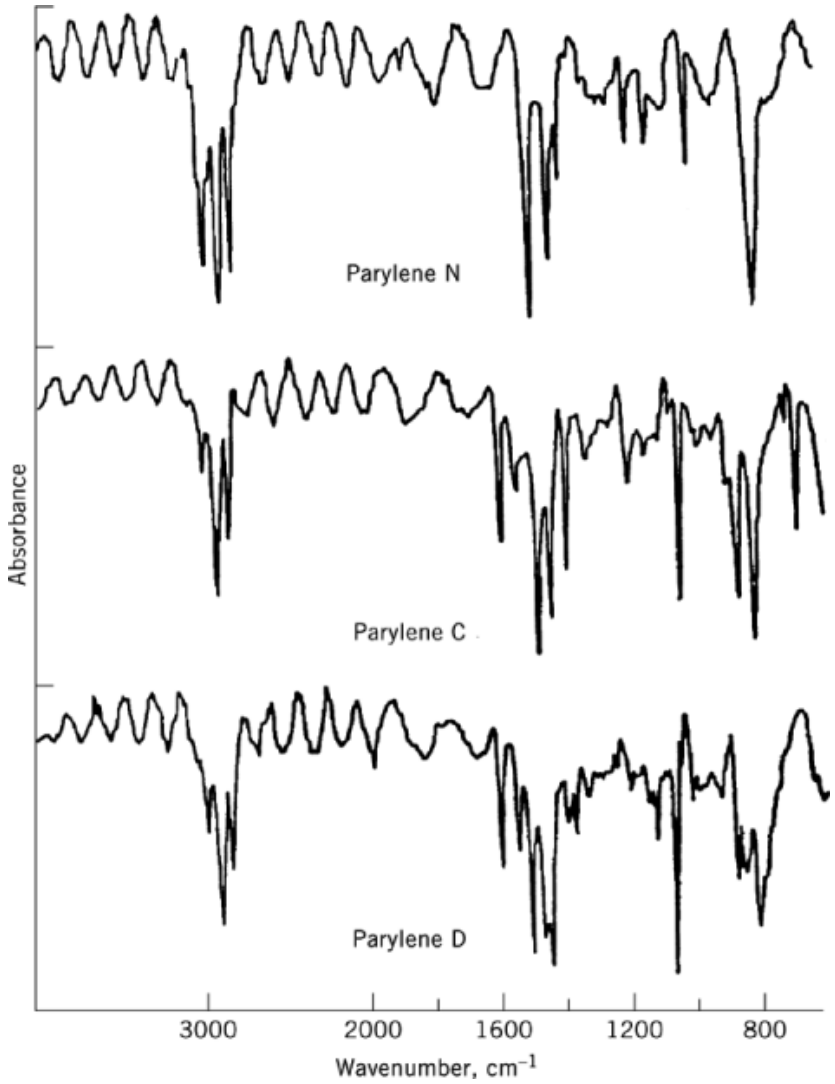

Fig. 12. Infrared absorption spectra of Parylenes N, C, and D films of 18-μm thickness.

film plane. Because the polymer chain is oriented along the c axis of the unit cell with the benzene rings lying approximately in the plane of the ⟨100⟩ face, it follows that, at least in among molecules within crystallites, there is a preference for the polymer chains and benzene rings to be oriented in the film plane. Within the film plane, however, the direction of the chains is random. That benzene rings are preferentially oriented in the plane of the film is supported by negative birefringence and by the Raman spectrum of the polymer (49).

5.2.9. Solvent Resistance

At temperatures below the melting of the crystallites, the parylenes resist all attempts to dissolve them. Although the solvents permeate the continuous amorphous phase, they are virtually excluded from the crystalline domains. Consequently, when a parylene film is exposed to a solvent a slight swelling is observed as the solvent

Table 6. Swelling on Immersion in Various Solvents for the Commercial Parylenes at Room Temperature

	Volume change, %		
Solvent	Parylene N	Parylene C	Parylene D
dichlorobenzene	0.2	3.0	1.8
mixed xylenes	1.4	2.3	1.1
monochlorobenzene	1.1	1.5	1.5
2,4-pentanedione	0.6	1.2	1.4
trichloroethylene	0.5	0.8	0.8
acetone	0.3	0.9	0.4
pyridine	0.2	0.5	0.5
isopropyl alcohol	0.3	0.1	0.1
Freon	0.2	0.2	0.2
water, deionized	0.0	0.0	0.0

invades the amorphous phase. In the thin films commonly encountered, equilibrium is reached fairly quickly, within minutes to hours. The change in thickness is conveniently and precisely measured by an interference technique. As indicated in Table 6, the best solvents, specifically those chemically most like the polymer (eg, aromatics such as xylene), cause a swelling of no more than 3%.

6. Applications

Although there is ample evidence in the literature that several industrial groups had a research interest in the PPXs during the 1950s, industrial exploitation was for the most part prevented by the obstacle the parylenes present to conventional fabrication technologies. Because they are generally insoluble in most solvents, even at elevated temperatures, they cannot be used as solvent-based coatings; neither can they be cast as films nor spun as fibers from solution. Because of their high crystalline melting points, melt-working (molding, extrusion, calendering, etc) is also difficult. Yet it is often just these features of solvent resistance and high temperature mechanical strength that constitute the advantages of PPX materials.

It had been recognized from the outset that polymer forms spontaneously on surfaces exposed to the gaseous monomer PX, but the recognition of VDP as an industrially viable process was not immediate. The public announcement, in 1965, of the convenient generation of pure monomer by the Gorham process from the dimer marked the beginning of a period of a gradually increased understanding and acceptance of the unique features of the parylenes.

As a coating technique, VDP offers certain advantages over other coating techniques such as brushing, dipping, or spraying. These advantages stem principally from the fact that the solid coating is formed from the gaseous monomer directly, without an intermediate liquid stage. As a result, the forces of surface tension, which would cause a pulling away from sharp edges and a filling in of troughs in conventional methods, are not operative and therefore do not affect the cross-sectional profile of VDP coatings. Coatings of PPX grow from the substrate surface outward, producing a conformal layer of uniform thickness. Extensive tests (50) demonstrate that the coating so formed is pinhole-free at thicknesses well below those achievable with conventional coating techniques (see Coatings).

The PPX coatings are formed spontaneously on substrates at or near room temperature; a cure cycle at elevated temperature is not necessary to complete the polymerization chemistry. The substrate need not be subjected to any temperatures above ambient, and no further time is required beyond that needed for the growth of the film. Because the polymerization is spontaneous, no catalyst is necessary. Catalysts that promote other polymerizations are often ionic or ionogenic and, to the extent that they remain in the coating after

cure, their residues are capable of participating in charge mobilization, with resulting detrimental effects in electrical properties. Because the coating is formed at room temperature, stresses that might be induced by differential thermal expansion between the temperature of cure and room temperature are avoided. Because PPX coatings are generally much thinner than conventional coatings, any stress that they impart on the substrate is proportionately less.

6.1. Circuit Boards

The most important application of parylenes is as a conformal coating for printed wiring assemblies. The parylene VDP process has the ability to produce a continuous, thin, truly conformal coating on geometrically complex, delicate articles. These coatings provide excellent chemical resistance, especially to solvent attack, and resistance to fungal attack. In addition, they exhibit stable dielectric properties over the wide range of temperatures in which military boards are expected to perform, as well as low dielectric constants, which together with thinness minimize the undesirable loading of high frequency tuned circuits. The reliability with which the process operates substantially reduces labor-intensive touch-up and inspection operations otherwise required for conventional coatings.

Parylene C was included among the earliest MIL-I-46058 (51) qualified coatings (as type XY) and has since enjoyed a reputation for superior performance in protecting and preserving the operation of electronic circuits against the detrimental effects of their operating environments. Environmental water is, of course, chief among these adverse factors. Although the rate of water transport through a parylene coating is finite and well documented, the hydrophobic nature of the parylenes makes them excellent barriers to penetration by ionic species. Once the circuit board is clean to the extent that surface ionic contamination is minimized and weak surface layers are eliminated, the parylene coating adheres well to the organic substrate material between the conductors. Ionic conduction along the coating–substrate interface, which would otherwise impair electrical performance in the short run and promote galvanic corrosion and dendritic growths in the long term, is minimized.

The sem photographs of Figure 13 show a conventional FR-4 printed wiring board, coated with an 8-μm film of Parylene C, on which the copper conductor trace has been peeled back. The peeling reveals the rough texture of the epoxy gel coat produced during the original lamination against etched copper in order to achieve maximum laminate peel strength. The region covered with Parylene C in Figure 13 was of the same texture before coating, a fact that, along with parylene's conformality, accounts for much of the texture in the upper surface. Of particular interest is the mode of Parylene C failure as the conductor is peeled. There is evidence of substantial yield prior to failure in the filamentous nature of the failed regions and the web of stretched Parylene C at the apex of the peel. Furthermore, all tensile failure is cohesive, ie, the adhesion of Parylene C to the underlying epoxy gel coat is greater than the cohesive strength within the coating material. The higher magnification (Fig. 13**b**) shows the line of demarcation between the regions covered with copper and with Parylene C prior to the peel, revealing that the breadth of the failed Parylene C exceeded by far its original thickness.

The circuit board with all its components attached presents a variety of surface types for the conformal coating, ranging from plastics through ceramics and glass to metals, in particular aluminum and tin–lead solder. No single mechanism for adhesion can serve all sites effectively. Of particular importance for the epoxy board are the surfaces between conductor traces. Because epoxy is an organic material that is permeable to PX monomer, the growth mechanism of the parylene coating provides adhesion by the interpenetrating network it produces. Care must be taken in cleaning the board surface before coating of leakage-producing ionic contamination as well as organic soils, which interfere with a secure xylylene interpenetration lock. In the cases of ceramic and metal surfaces, monomer penetration is impossible, and other adhesion mechanisms must be engaged. Adhesion to metals is often not essential to the performance of the board, but it is usually desirable. Adhesion to ceramics or glasses is vital in situations where electrical leakage across their surfaces is to be minimized,

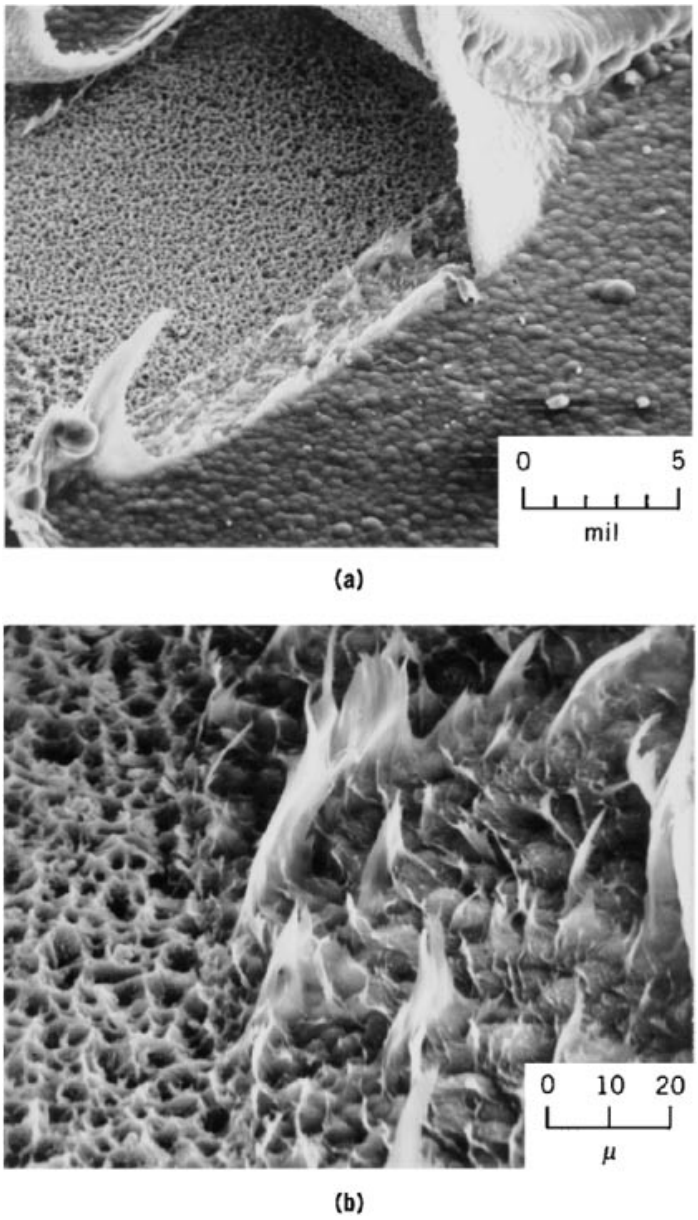

Fig. 13. Scanning electron microscope (sem) photographs of Parylene C-coated printed circuit conductor peeled to demonstrate the adhesion of the coating to the substrate. To convert mil to meters, multiply by 2.54×10^{-5}.

and is particularly necessary in hybrids. Because the outside surface of common metals is an adherent coating of native oxide, adhesion to metals, ceramics, and glasses can often be achieved using the same approach, ie, treatment with a compatibilizing layer of an organosilane (52). γ-Methacryloxypropyltrimethoxysilane (A-174) is the organosilane most commonly used for the purpose. In action, the trialkoxysilane end of the molecule hydrolyzes and bonds covalently with the oxide on the substrate surface. The methacrylic end of the

molecule provides a hydrophobic surface to accommodate parylene deposition, as well as the opportunity to form covalent bonds with the *p*-xylylene polymer through its double bond. It is, of course, essential to provide no more than a monolayer of the organosilane. Water plays an important role in the bonding chemistry between the organosilane and the oxide, and the treatment is often applied from aqueous solution. An alternative treatment is by exposure of the substrate circuit boards to pure gaseous organosilane (53), a process which often takes several days to develop optimum adhesion.

Fluorescence is frequently required in a circuit-board coating to assist inspection of the board after it is coated. Fluorescent parylene coatings can be prepared by admixing a fluorescent agent into the dimer charge. The agent must have just the right volatility to pass through the process and deposit with the polymer, yet it must be sufficiently stable that it survives the conditions it encounters during the process. Agents that have been used in this manner are anthracene and certain fluorescent whiteners of the Calcofluor family, the 7-dialkylamino-4-methylcoumarins (see Fluorescent whitening agents).

6.2. Hybrid Circuits

The use of parylenes as a hybrid circuit coating is based on much the same rationale as its use in circuit boards. A significant distinction lies in obtaining adhesion to the ceramic substrate material, the success of which determines the eventual performance of the coated part. Adhesion to the ceramic must be achieved using adhesion promoters, such as the organosilanes.

In the coating of hybrid circuits, parylene provides certain other advantages. In certain technologies, chips are mounted with substrate clearances of as little as 10 μm. The parylene VDP process penetrates this narrow space, coating the underside of the chip as well as the substrate opposite it. Conventional coatings cannot flow into such a narrow space and must rely on simply sealing it off, leaving an air pocket under the chip. Where the fabrication technology uses wire bonds to connect the chips with substrate conductor patterns electrically, the fine (25-μm dia) wires are coated by the parylene VDP process to the same thickness as all other surfaces. A marked increase in wire-bond strength in pull tests on coated hybrids is observed. The increase in strength can be attributed to the strengthening effect of the coating on the wire (which typically exceeds in cross section the amount of metal in the wire) or to a reinforcement of the welded junction to the chip pad or substrate conductor.

A hybrid solid-state relay needed for a NASA space experiment underwent redesign to provide 2500-V d-c isolation, input-to-output, while undergoing temperature cycling from -120 to $+180^{\circ}\mathrm{C}$, as detailed in an instructive published case history (54). The electrical isolation requirement was met only by using a conformal coating, although several conventional coatings were evaluated along with parylene. These stresses in the thicker conventional coatings associated with temperature excursions resulted, in all cases other than parylene, in the rupture of the circuitry and the functional failure of the relay.

During the manufacture of hybrid circuits, it is possible to generate small metallic fragments such as wire chips and solder balls. If they are not removed before hermetic packaging, they can disrupt performance of the unit at some future time. In certain aerospace or military applications where no physical replacement of the unit is possible, such a failure could mean the loss of a mission. A program intended to improve the reliability of hermetic packages in critical systems concluded by finding a solution to this problem by applying a parylene coating to the inside of the hybrids. The coating confers electrical insulation to all surfaces and tends to anchor any loose particles; it also confers nonconductance should they break loose from their moorings. From the standpoint of coating technology, the most interesting part of this solution to the particle-immobilization problem is the throwing power, demonstrated by the fact that the entire internal surface of the hybrid is coated through a 0.5–1.0-mm hole in the lid of the hermetic package (55).

6.3. Semiconductors

The distinctive conformality of parylene is often regarded as a handicap for meeting the requirements of an interlayer dielectric (ILD) in large-scale integration (LSI) multilevel interconnection systems. After many layers of successive patterning, a planarizing procedure is very much needed, not a procedure that would replicate the existing lumpiness. A polyimide, the first organic compound to be used in a commercial semiconductor structure, was selected for this application (56), because of the planarization inherent in its spinning application procedure. However, because parylene offers distinct advantages in purity and thickness control and low moisture absorption (particularly in comparison to the polyimides), it receives continued attention in the search for new fabrication techniques (57). Recognition of the need to lower the dielectric constant of ILD insulating materials as a means of improving device performance has generated a renewed interest in organics in general, and the parylenes in particular. To meet this opportunity, the intent to produce the dimer of the per-α-fluorinated version known as Parylene AF4 (poly(α,α,α',α'-tetrafluoro-*p*-xylylene)) [74952-03-7] has been announced (58). In addition to offering a dielectric constant in the vicinity of 2.35, its thermal stability is such that it can withstand back-end-of-line processing steps at temperatures up to 450°C without perceptible weight loss.

In an interesting extension of the conventional solid-state device concept, where a thin film covers the channel of a field-effect transistor (FET), the electron current in the channel may be made to respond to changes in the chemical environment on the opposite side of the film. Thus a silicon nitride film on a channel gives an ion-selective FET (ISFET) that responds to the pH of a solution with which it is in contact. The hydrophobic nature of parylene, on the other hand, enables the channel it covers to be independent of solution composition, and such a channel can be used as a reference electrode. An important advantage of parylene in this context is the thinness with which it can be deposited as a continuous film. The gate coatings are 0.1 μm thick, a thinness required if the sensor is to have a speedy response. An experimental probe-type all-solid-state pH sensor has been demonstrated (59). It was also demonstrated that chemically modifying the parylene surface with crown ether compounds can give an ISFET (known as a CHEMFET) that responds to potassium ion concentration.

Sensors for physical effects are also fabricated using standard semiconductor technology. A notable example is a silicon membrane pressure transducer, which, among its many other uses, is currently employed as a manifold pressure transducer in automobiles (60). The thin membrane of single-crystal silicon was prepared by etching most of the wafer thickness away, into which a resistive Wheatstone Bridge network that enables an electrical readout of the membrane's physical strain while flexing had previously been diffused. Although it is desirable to insulate the membrane electrically from the medium it measures, it is also desirable to do so without affecting the elasticity of the membrane, so that it retains its calibration of electrical output vs input pressure. A thin coating of Parylene C easily accomplishes both. In an inversion of roles, these same pressure transducers were used to sense the stresses imparted to coated substrates by a variety of MIL-I-46058C qualified coating materials (61). Whereas all other coatings, as a result of their cure shrinkages acting through their greater thicknesses modified by their assorted elastic moduli, affected sensor calibration in all cases, the presence of 13 μm of Parylene C was barely detectable.

6.4. Capacitors

The outstandingly low dielectric loss of parylenes make them superior candidates for dielectrics in high quality capacitors. Furthermore, their dielectric constant and loss remain constant over a wide temperature range. In addition, they can be easily formed as thin, pinhole-free films. Kemet Flatkaps are fabricated by coating thin aluminum foil with Parylene N on both sides and winding the coated foils in pairs (62).

Parylenes are also used to coat the rotor and stator plates of miniature variable air-gap tuning capacitors (63). Coating the plate raises the voltage that must be applied between two parallel plates for a discharge to occur in the air gap. Thus, a closer plate spacing is permitted, and a smaller unit having the same electrical

function can be built. This is also beneficial in improving design capacitance per unit volume. Compared to the alternative of interleaving dielectric films between the plates, the coated-plate technique offers the advantages of simplicity in assembly as well as reliability of the unit. Uniformity and thickness control are of paramount importance in this case.

6.5. The Bathythermograph

The thermistor sensing probe of a disposable bathythermograph is coated with parylene. This instrument is used to chart the ocean water temperature as a function of depth. Parylene provides the needed insulation resistance and is thin and uniform enough to permit a rapid and accurate response to the temperature of the surrounding salt water (64).

6.6. Miniature Electrical Components

In the manufacture of miniature transformers and motor armatures, it is often necessary that the winding be electrically isolated from the bobbin. The insulating varnish of fine copper wire often does not survive the rigors of the winding operation, and, particularly in the case of the smaller devices, the bobbin requires insulation. However, a thicker insulation than is absolutely necessary takes up space that otherwise could be used for more turns of wire. Thus, thickness control in the coating of the bobbin means better performance of the finished device. Parylene is used in the manufacture of high quality miniature stepping motors, such as those used in wristwatches, and as a coating for the ferrite cores of pulse transformers, magnetic tape-recording heads, and miniature inductors, where the abrasiveness of the ferrite is particularly damaging. In the coating of complex, tiny objects such as these, the VDP process has an extra labor-saving advantage. It is possible to coat thousands of such articles simultaneously by tumbling them during the VDP operation (65).

6.7. Medical Uses

Under the auspices of the National Institutes of Health Artificial Heart program (66), Parylene C received considerable attention as a component of a novel scheme for achieving blood compatibility in a flexible pump chamber wall by anchoring the endothelial tissue of the host to it. A microfiber nonwoven fabric anchored to the flexible wall by an overcoating of Parylene C provides scaffolding for cellular ingrowth (67). Although the scheme is not used today, the program contributed a significant amount of favorable biocompatibility data on Parylene C, particularly in the area of cytotoxicity (68). Parylene's minimal perturbance of cells growing in its vicinity can be ascribed to its high purity and its ability to slow down impurity species that might otherwise diffuse out of a substrate material. The corrosive biological environment does not affect parylene, which cannot be hydrolytically degraded.

Parylene's use in the medical field is linked to electronics. Certain pacemaker manufacturers use it as a protective conformal coating on pacemaker circuitry (69). The coated circuitry is sealed in a metal can, so that the parylene coating serves only as a backup should the primary barrier leak. There is also interest in its use as an electrode insulation in the fabrication of miniature electrodes for long-term implantation to record or to stimulate neurons in the central or peripheral nervous system, as the "front end" of experimental neural prostheses (70). One report describes the 3-yr survival of functioning parylene-coated electrodes in the brain of a monkey (71).

6.8. Artifact Conservation

As books age, the paper of their pages becomes brittle. A relatively thin coating of parylene can make these embrittled pages stronger (72). Parylene coats the fibers conformally and welds them together at crossing

points, providing added structural strength. Although parylene does little to retard the chemical processes that make the paper brittle, it restores some physical strength. Furthermore, the parylene coating can be applied to the existing book without disturbing the binding, thus saving the labor of disassembly. The concept has been extended to other fragile artifacts, such as fabrics.

6.9. Laser Fusion Targets

In the search for new energy sources, some research is directed toward the thermonuclear fusion of deuterium–tritium (DT) mixtures. In laser-driven inertial confinement fusion, a single laser pulse crushes a target containing the DT fuel to one thousandth of its normal volume and achieves a temperature of 10^8 K. The energy per pulse in current lasers is small, which limits the experimental targets to a diameter of about 100 μm. The outer layer of the spherical target absorbs the omnidirectionally incident laser energy and ablates as it is thermally destroyed, imparting a reactive compressive force on the inner portions of the target, thus compressing it. The dimensions of the outer layer are central to achieving hydrodynamic stability during the implosion process. Concentricity, sphericity, and thickness (ca 10 μm) must be better than 5%, and surface roughness must be no greater than 0.1 μm. Parylene is a leading contender for the outer layer, and considerable ingenuity has been applied in several methods for experimental target fabrication (73).

6.10. Contamination Control

In a number of developing technologies, contamination by small particles is a serious problem. To the extent that the generation of freely mobile particles is reduced by securing them to their initial locations, parylene coating of critical system components can be useful. In the manufacture of Winchester disk drive units, large magnesium castings are coated with parylene. This increases system reliability (74), presumably because the large surface within the sealed unit, if not coated, is capable of producing particles of the same destructive potential that the system seal is supposed to prevent from entering.

6.11. Barrier Coating

The bulk permeabilities of parylenes, although finite, are generally lower than those of most other types of plastic materials. The further advantage of coating continuity inherent in the VDP process allows the parylenes to realize the benefits of their low permeabilities to the fullest, without leakage of the permeant through coating defects such as cracks or pinholes. Thus the parylenes are uniquely suited as protective encapsulants or barrier coatings (see Barrier polymers).

Where pieces of lithium metal are coated with Parylene C, and their subsequent reaction to water vapor follows, the steady-state generation of hydrogen can be controlled exactly by the rate of water transport through the coating (75). Pellets of nitronium perchlorate, a potent oxidizer useful as a solid-rocket propellant component, can be rendered less moisture-sensitive and compatible with organic binders by applying a coating of Parylene C (76). The absorption of water by particulate ammonium nitrate could be reduced tenfold by as little as a 0.7% coating of Parylene C (77). Particles of ammonium nitrate remain free-flowing after long exposures to ambient conditions of temperature and moisture when coated with as little as 0.2% Parylene C. The thermal sensitivity of Parylene C-coated ammonium nitrate (time to explosion) is unaffected by the coating. On the other hand, the 1.5–8% coating of particulate military-grade RDX explosive, cyclotrimethylene trinitramine, produced significant changes in physical and explosive properties. The changes were attributed to the chemical properties of the protective Parylene C coating and to the virtual absence of encapsulated agglomerates of RDX crystals (78).

In a recent report (79), a 150–200 mg/cm^2 Parylene C coating provided protection against moisture uptake by three-phase, polyimide, microballoons, and air, syntactic foams. In a previously reported coating of a similar foam, the stated purpose was strengthening (80).

6.12. Corrosion Control

The oxygen and water permeability and thinness of the parylene coatings notwithstanding, the rate of corrosion of a coated surface is often significantly reduced. In one case, the corrosion of a plated wire memory was reduced to the point where no bits were lost during 30 cycles of a MIL STD 202D-106C test by overcoating the permalloy plating, which had been previously coated with a Ni–P anticorrosive layer, with Parylene N (81).

6.13. Dry Lubricant

The static and dynamic coefficients of friction for the parylenes are low and virtually the same. This feature is an advantage in the use of a parylene coating as a dry lubricant on the bearing surfaces of miniature stepping motors. Coating a threaded ferrite core significantly reduces the abrasion to coil forms (82).

6.14. Pellicles and Membranes

By separating the coating from the substrate after deposition, the unique coating features of parylenes, especially continuity and thickness control and uniformity, can be imparted to a freestanding film. In practice, a sheet of smooth glass is coated with a layer of a hygroscopic substance before being coated with parylene. The film is then lifted from the glass by water immersion to activate the release agent. In this manner, uniform, continuous, freestanding parylene films with thicknesses of less than 0.1 μm can be prepared. Applications of such films include optical beam splitters (83), a window for a micrometeoroid detector (84), a detector cathode for an x-ray streak camera (85), windows for x-ray proportional counters (86), a charge stripper for converting a portion of the H-output beam of a 50 MV LINAC to neutral H^0 for diagnostic purposes (87), and a massless support for projectile abrasion testing (88); proposals have included the membrane structure for a solar sail (89).

7. Health and Safety

In a world increasingly conscious of the dangers of contact with chemicals, a process that is conducted within the walls of a vacuum chamber, such as the VDP process for parylene coatings, offers great advantages. Provided the vacuum pump exhaust is appropriately vented and suitable caution is observed in cleaning out the cold trap (trace products of the pyrolysis, which may possibly be dangerous, would collect here), the VDP parylene process has an inherently low potential for operator contact with hazardous chemicals.

To an experienced operator trained in the handling of industrial chemicals, the dimers present little cause for concern in handling or storage. The finished polymer coating presents even less of a health problem; contact with the reactive monomer is unlikely. In the ancillary operations, such as cleaning or adhesion promotion, the operator must observe suitable precautions. Before using the process chemicals, operators must read and understand the current Material Safety Data Sheets, which are available from the manufacturers.

BIBLIOGRAPHY

"Xylylene Polymers" in *ECT* 3rd ed., Vol. 24, pp. 744–771, by S. M. Lee, Ford Aerospace and Communications Group.

Cited Publications

1. L. A. Errede and M. Szwarc, *Q. Rev. Chem. Soc.* **12**, 301 (1958); M. Szwarc, *Polym. Eng. Sci.* **16**(7), 473 (1976); W. F. Gorham and W. D. Niegisch "Xylylene Polymers" in N. M. Bikales, ed., *Encyclopedia of Polymer Science and Technology*, Vol. **15**, Interscience Publishers, a Division of John Wiley & Sons, Inc., New York, 1989, 98–124.
2. U.S. Pat. 3,342, 754 (Sept. 19, 1967), W. F. Gorham (to Union Carbide Corp.).
3. W. F. Gorham, *J. Polym. Sci. A-1* **4**, 3030 (1966).
4. W. F. Gorham, *J. Polym. Sci. A-1* **4**, 3027 (1966).
5. R. B. Woodward and R. Hoffmann, *The Conservation of Orbital Symmetry*, Chapt. 6, pp. 70, 85, and reference 96 therein.
6. L. K. Montgomery and co-workers, *J. Am. Chem. Soc.* **108**(19), 6004 (1986).
7. P. G. Mahaffy, J. D. Wieser, and L. K. Montgomery, *J. Am. Chem. Soc.* **99**(13), 4514 (1977).
8. U.S. Pat. 4,532,369 (July 30, 1985), H. Hartner (to Merck); U.S. Pat. 4,769,505 (Sept. 6, 1988), C. Lee and D. R. Bassett, (to Union Carbide Corp.).
9. D. J. Williams, J. M. Pearson, and M. Levy, *J. Am. Chem. Soc.* **92**, 1436 (1970).
10. S. K. Pollak, B. C. Raine, and W. J. Hehre, *J. Am. Chem. Soc.* **103**(21), 6308 (1981).
11. M. J. S. Dewar, *J. Am. Chem. Soc.* **104**(5), 1449 (1982).
12. H. G. Gilch, *J. Polym. Sci. A-1* **4**, 438–439 (1966).
13. V. V. Korshak and S. L. Sosin, *Vysokomol. Soyed.* **7**(2), 232–238 (1965).
14. U.S. Pat. 3,787,382 (Jan. 22, 1974), A. N. Wright, W. R. Burgess, and E. V. Wilkus, (to General Electric Co.); M. Inoue, H. Fujioka, T. Sorita, and T. Tanaka, *ACS Polym. Preprints* **28**(2), 332 (1987).
15. Y. Takai, Y. Hayase, T. Mizutani, and M. Ieda, *J. Phys. D.* **17**, 399 (1984).
16. J. R. Salem, F. O. Sequeda, J. Duran, W. Y. Lee, and R. M. Yang, *J. Vac. Sci. Technol.* **A4**(3), 369 (1986); Y. Takahashi, M. Iijima, K. Inagawa, and A. Itoh, *ibid.* **A5**(4), 2253 (1987).
17. F. E. Arnold and L. S. Tan, *31st Int. SAMPE Symp.* **31**, 1185 (1986); U.S. Pat. 4,711,964 (Dec. 8, 1987), L. S. Tan and F. E. Arnold (to University of Dayton).
18. Y. Ito, S. Miyata, M. Nakatsuka, and T. Saegusa, *J. Org. Chem.* **46**, 1043 (1981).
19. Eur. Pat. 220,743 (May 6, 1987), R. Ungarelli, M. A. Baretta, and L. Sogli (to Montedison SpA).
20. Eur. Pat. 226,255 (June 24, 1987), R. Ungarelli, M. A. Baretta, and A. Malacrida (to Montedison SpA).
21. Eur. Pat. 220,744 (May 6, 1987), G. F. Pregaglia, M. A. Baretta, and A. Malacrida (to Montedison SpA).
22. C. J. Brown, *J. Chem. Soc.*, 3265 (1953).
23. R. H. Boyd, *Tetrahedron* **22**, 119 (1966); D. L. Rodgers, E. F. Westrum, Jr. and J. T. S. Andrews, *J. Chem. Thermodyn.* **5**, 733–739 (1973).
24. D. E. Kirkpatrick, Ph.D. dissertation, Rensselaer Polytechnic Institute, Troy, N.Y., 1984.
25. M. Gazicki, G. Surendran, W. James, and H. Yasuda, *J. Polym. Sci. Polym. Chem. Ed.* **23**, 2255 (1985).
26. H. Sawada, *Thermodynamics of Polymerization*, Marcel Dekker, Inc., New York, 1976.
27. M. Souders and co-workers, *Ind. Eng. Chem.* **41**, 1048 (1949).
28. D. R. Stull, E. F. Westrum, Jr., and G. C. Sinke, *The Chemical Thermodynamics of Organic Compounds*, Krieger, Malabar, Fla., 1987, p. 699.
29. D. E. Kirkpatrick, L. Judovits, and B. Wunderlich, *J. Polym. Sci. Polym. Phys. Ed.* **24**, 45 (1986).
30. R. W. Warfield and M. C. Petree, *J. Polym. Sci.* **55**, 497 (1961).
31. S. Y. Lazareva, *Vysokomol. Soedin.* **A21**(7), 1509 (1979).
32. B. L. Joesten, *J. Appl. Polym. Sci.* **18**, 439 (1974).
33. W. A. Alpaugh and D. R. Morrow, *Thermochim. Acta* **9**, 171 (1974).
34. W. F. Beach, *Macromolecules* **11**(1), 72 (1978).
35. F. E. Cariou, D. J. Vally, and W. E. Loeb, *IEEE Trans. Parts Mater. Packag.* **PMP-1**(1), 54 (1965).
36. J. F. Gaynor, S. B. Desu, and J. J. Senkevich, *Macromolecules* **28**, 7343–7348 (1996).
37. B. J. Bachman, *Proceedings of the 1st International SAMPE Electronics Conference*, Santa Clara, Calif., June 23–25,

1987, 431–440.
38. A. von Hippel, in E. U. Condon, and H. Odishaw, eds., *Handbook of Physics*, 2nd ed., McGraw-Hill Book Co., Inc., New York, 1968, Pt. 4, p. 104.
39. U.S. Pat. 4,163,828 (Aug. 7, 1979); U.S. Pat. 4,173,664 (Nov. 6, 1979), G. S. Cieloszyk (to Union Carbide Corp.); U.S. Pat. 4,176,209 (Nov. 27, 1979), T. E. Baker, G. L. Fix, and J. S. Judge (to Raytheon); T. E. Nowlin, D. F. Smith, and G. S. Cieloszyk, *J. Polym. Sci. Polym. Chem. Ed.* **18**(7), 2103 (1980); T. E. Baker, G. L. Fix, and J. S. Judge, *J. Electrochem. Soc.* **127**(8), 1851 (1980).
40. W. H. Hubbel, Jr., H. Brandt, and Z. A. Munir, *J. Polym. Sci. Polym. Phys. Ed.* **13**, 493 (1975).
41. E. Sacher, *J. Appl. Polym. Sci.* **28**, 1535 (1983).
42. R. S. Corley, H. C. Haas, M. W. Kane, and D. I. Livingston, *J. Polym. Sci.* **13**, 137 (1954).
43. T. E. Nowlin and D. F. Smith, *J. Appl. Polym. Sci.* **25**, 1619 (1980).
44. D. E. Kirkpatrick and B. Wunderlich, *J. Polym. Sci. Polym. Phys. Ed.* **24**, 931 (1986).
45. R. Iwamoto and B. Wunderlich, *J. Polym. Sci. Polym. Phys. Ed.* **11**, 2403 (1973).
46. S. Isoda, M. Tsuji, M. Ohara, A. Kawaguchi, and K. Katayama, *Polymer* **24**, 1155 (1983).
47. S. Isoda, T. Ichida, A. Kawaguchi, and K. Katayama, *Bull. Inst. Chem. Res. Kyoto Univ.* **61**(3), 222 (1983).
48. W. D. Niegisch, *J. Appl. Phys.* **38**(11), 4110 (1967).
49. M. S. Mathur, and G. C. Tabisz, *J. Cryst. Mol. Struct.* **4**, 23 (1973).
50. M. A. Spivack and G. Ferrante, *J. Electrochem. Soc.* **119**(11), 1592 (1969).
51. *MIL-I-46058C(6): Insulating Compound, Electrical (for Coating Printed Circuit-Assemblies)*, U.S. Dept. of Defense, Washington, D.C., Nov. 8, 1982.
52. U.S. Pat. 3,600,216 (Aug. 17, 1971), D. D. Stewart (to Union Carbide Corp.).
53. Ger. Pat. 2,737,792 (Mar. 2, 1978), D. M. Mahoney and W. F. Beach (to Union Carbide Corp.).
54. B. L. Slater, T. J. Riley, and W. Janssen, *Proceedings of the IEEE Power Electronics Specialists Conference*, Pasadena, Calif., June 11–13, 1973, 163–169.
55. V. S. Kale and T. J. Riley, *IEEE Trans. Parts Hybrids Packag.* **PHP-1**(3), 273 (1977).
56. D. L. Bergeron, J. P. Kent, and K. E. Morrett, *22nd Proceedings of the International Reliability Physics Symposium*, Las Vegas, Nev., 1984, 229–233.
57. J. M. Baker, J. H. Magerlein, and M. J. Palmer, *IBM Tech. Disel. Bull.* **27**(7B), 4382 (Dec. 1984); Jpn. Pat. 62 106456 (Nov. 1, 1986), M. Kanazawa and S. Kawanako, (to Fujitsu, Ltd.); W. F. Beach and T. M. Austin, *Hybrid Circ. Technol.*, 33–36 (Jan. 1990).
58. J. Wary, R. A. Olson, and W. F. Beach, *2nd International Dielectrics for VLSI/ULSI Multilevel Insulation Conference (DUMIC)*, Santa Clara, Cal., Feb. 20–21, 1996, 207–213.
59. T. Matsuo, H. Nakajima, T. Osa, and J. Anzai, *Sensors Actuat.* **9**(2), 115 (1986).
60. R. Olson, *Electron. Packag. Prod.*, 213 (May 1980).
61. R. Olson, *Circuits Mfg.*, 57 (Jan. 1986).
62. U.S. Pat. 3,327,184 (June 20, 1967), D. J. Valley (to Union Carbide Corp.); U.S. Pat. 3,319,141 (May 9, 1967), F. E. Cariou, W. E. Loeb, and D. J. Valley (to Union Carbide Corp.).
63. U.S. Pat. 3,949,280 (Apr. 6, 1976), S. Odagiri, M. Nuka, N. Shinba, M. Baba, and Y. Iizuka (to Mitsumi Electric Co., Ltd.); Ger. Pat. 2,546,332 (Apr. 29, 1976), J. Lefeber and J. deJonge (to N. V. Philips Gloeilampenfabriken).
64. U.S. Pat. 3,389,604 (June 25, 1968), G. B. Williams (to Buzzards Corp.).
65. Ger. Pat. 2,329,186 (Jan. 3, 1974), F. R. Tittmann (to Union Carbide Corp.); U.S. Pat. 3,300,332 (Jan. 27, 1967), W. F. Gorham and H. L. Willard (to Union Carbide Corp.).
66. *Contract No. N01-HV-8-1388*, National Heart, Lung and Blood Institute, Division of Heart and Vascular Diseases, Bethesda, Md.
67. F. R. Tittmann and W. F. Beach in M. Szycher and W. J. Robinson, eds., *Synthetic Biomedical Polymers: Concepts and Applications*, Technomic Publishing Co., Inc., Westport, Conn., 1980, 117–132.
68. R. H. Kahn and W. E. Burkel, *In Vitro* **8**(6), 451 (1973).
69. R. Olson, *Electron. Packag. Prod.*, 213 (May 1980).
70. E. M. Stemmed, *J. Electrophysiol. Tech. Eng.* **10**(1), 19 (1983); G. E. Loeb, M. Salcman, and E. M. Schmidt, *IEEE Trans. Bionwd. Eng.* **BME-24**(2), 121 (1977).
71. E. M. Schmidt, J. S. McIntosh, and M. J. Bak, *Med. Biolog. Eng. Comput.*, 96 (Jan. 1988).
72. B. J. Humphrey, *J. Am. Inst. Conserv.* **25**(6), 15 (1986); C. J. Shahani and W. K. Wilson, *Am. Sci.* **75**(3), 240 (1987).

73. D. F. Peiffer, T. J. Corley, G. M. Halpern, and B. A. Brinker, *Polymer* **22**(4), 450 (1981); R. Q. Gram, H. Kim, J. F. Mason, and M. Wittman, *J. Vac. Sci. Technol.* **A4**(3), 1145 (1986); K. W. Beig, *J. Vac. Sci. Technol.* **18**(3), 1231 (1981); U.S. Pat. 4,381,963 (May 3, 1983), I. S. Goldstein, F. D. Kalk, and H. W. Deckman (to The University of Rochester).
74. R. Olson and R. Veague, *Microcontamination*, 57 (Jan. 1985).
75. M. A. Spivack, *Corrosion (Houston)* **26**(9), 371 (1970).
76. U.S. Pat. 3,523,839 (Aug. 11, 1970), L. Shechter and W. E. Loeb (to Union Carbide Corp.); U.S. Pat. 3,556,881 (Jan. 19, 1971), W. F. Gorham and W. E. Loeb (to Union Carbide Corp.).
77. T. C. Castorina and A. F. Smetana, *J. Appl. Polym. Sci.* **18**, 1373 (1974).
78. A. F. Smetana and T. C. Castorina, *Proceedings of the Propellants, Explosives and Pyrotechnics Conference*, Dec. 3–4, 1974, Picatinny Arsenal, Dover, N.J.
79. A. Calahorra, O. Gara, and S. Kenig, *J. Cell. Plast.* **23**(7), 383 (1987).
80. R. J. McWhirter, *Report from Bendix Corp.*, BDX-613-2358, Bendix Corp., Kansas City, Mo., Sept. 1980.
81. K. Makino, S. Kawakami, and S. Orihara, *Fujitsu Sci. Tech. J.* **9**(4), 153 (1973).
82. R. Olson, *Electron. Packag. Prod.*, 213 (May 1980).
83. M. A. Spivack, J. N. Pike, and W. M. Jayne, *Proceedings of the Electro-Optical Systems Design Conference*, New York, N.Y., Sept. 18–20, 1973, 362–371.
84. N. Pailer and E. Grun, *Planet. Space Sci.* **28**(3), 321 (1980).
85. P. L. Tassano, *J. Vac. Sci. Technol.* **A3**(5), 2036 (1980).
86. P. H. Sheather, *J. Physics E.* **6**(4), 319 (1973).
87. S. L. Kramer and D. R. Moffett, *IEEE Trans. Nucl. Sci.* **NS-28**(3), 2174 (1981).
88. U.S. Pat. 3,940,530 (Feb. 24, 1976), W. E. Loeb and M. A. Spivack (to Union Carbide Corp.); U.S. Pat. 3,864,202 (Feb. 4, 1975).
89. U.S. Pat. 4,321,299 (Mar. 23, 1982), R. A. Frosch and R. A. Frazer (to NASA).

W. F. BEACH
Alpha Metals

Related Articles

Semiconductors; Integrated circuits; Coating